PHOTOLUMINESCENCE SPECTROSCOPY OF 4H- AND 6H-SiC

THESIS

William A. Davis, 2nd Lieutenant, USAF

AFIT/GAP/ENP/94D

DEPARTMENT OF THE AIR FORCE
AIR UNIVERSITY
AIR FORCE INSTITUTE OF TECHNOLOGY

Wright-Patterson Air Force Base, Ohio

AFIT/GAP/ENP/94D-2

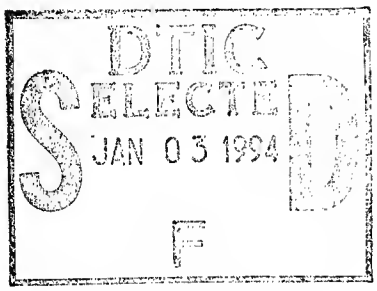

PHOTOLUMINESCENCE SPECTROSCOPY OF 4H- AND 6H-SiC

THESIS

William A. Davis, 2nd Lieutenant, USAF

AFIT/GAP/ENP/94D

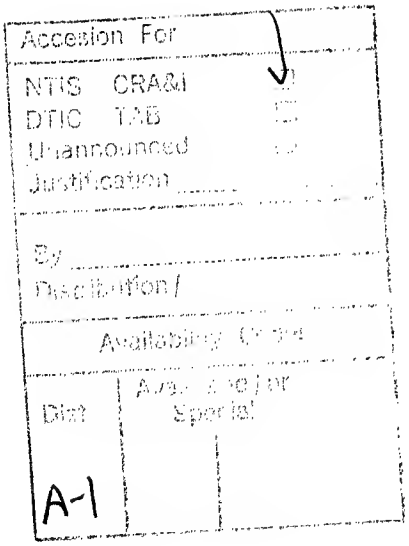

The views expressed in this thesis are those of the author and do not reflect the official policy or position of the Department of Defense or the U.S. Government.

AFIT/GAP/ENP/94D-2

PHOTOLUMINESCENCE SPECTROSCOPY OF 4H- AND 6H-SiC

THESIS

Presented to the Faculty of the School of Engineering

of the Air Force Institute of Technology

Air University

in Partial Fulfillment of the

Requirements for the Degree of

Master of Science in Engineering Physics

William A. Davis, B.S.

2nd Lieutenant, USAF

December 1994

Acknowledgments

I wish to take this time to thank the team of people who made this study possible. As in any project, there are numerous people who in some way or another contribute to the end product. I first would like to thank my advisor Dr. R. L. Hengehold for his guidance and suggestions throughout this project. I also thank Dr. William Mitchel of Wright Laboratory Materials Directorate for supplying me the SiC samples as well as the very helpful discussions. Without the help of Mr. Greg Smith this project would have gone nowhere and I am deeply indepted to him for his technical assistance. For their helpful discussions on luminescence in general and SiC, I would like to thank Captain Eric J. Silkowski and Mr. Jim Scofield. Finally, I must express my deepest appreciation for my best friend Joe, who is no longer with me physically, but his spirit lives on with me with the numerous conversations and shared experiences that I will never forget.

William A. Davis

Table of Contents

List of Tables

List of Figures

Abstract

Typical undoped bulk grown SiC shows n- or p-type conductivity due to residual impurities such as nitrogen, boron, or aluminum. In order to produce high resistivity material, vanadium can be used as a compensating dopant. Since vanadium is an amphoteric dopant in SiC, it produces either a donor state, $V_{Si}^{4+}(3d^1) \rightarrow V_{si}^{5+}(3d^0)$, or an acceptor state, $V_{Si}^{4+}(3d^1) \rightarrow V_{si}^{3+}(3d^2)$. Thus, vanadium doping can compensate both n- and p-type conductivity. In this work, vanadium doped and undoped 4H- and 6H-SiC grown by the sublimation method have been studied using low temperature photoluminescence (PL). It was found that the luminescence observed between 0.85 to 0.95 eV of the intra-3d-shell transition of $V_{si}^{4+}(3d^1)$ increased by an order of magnitude in samples intentionally doped with vanadium compared to samples unintentionally doped. In addition, the dominant visible-region luminescence was attributed to titanium which is an isoelectronic trap in SiC. The presence of a broad peak centered at ≈1.90 eV in some samples is believed to be attributed to donor-acceptor pair recombination between a Ti_{Si}-N_C complex donor and the boron defect complex acting as an acceptor. Finally, the Ti_{Si}-N_C complex donor location in the bandgap of 6H-SiC is estimated to be E_C-0.54 eV.

1. Motivation

1.1 High Temperature and High Power Electronics

Silicon Carbide (SiC) is a wide bandgap semiconductor that has potential for application in high temperature, high frequency, high voltage, and severe radiation environments. SiC's suitability for high temperature and high power applications is determined by its large bandgap, ≈3.0 eV for 6H-SiC, a maximum operating temperature of 600°C, and a breakdown voltage of 4×10^6 V/cm, over ten times as large as Si's.[1] Combined with excellent physical stability , SiC shows great promise as a high temperature semiconductor. The electron and hole mobilities, however, are not as high as Si's, but the values achieved to date, 600 and 40 cm^2/V s, are suitable for most electronic applications.

The Air Force has great interest in developing SiC devices for high temperature electronics for deployment in present and future weapon systems. In particular, aircraft electronics have been targeted as the main area of application for SiC devices. Over 90% of an aircraft's environmental control system is used to cool electronics; in addition, over 50% of all electronic failures in aircraft are attributed to electronic operating temperatures above military specifications. As aircraft and engine designs become more advanced, their operating temperatures will increase above the military specifications for Si of 125°C. SiC based electronics would improve reliability at higher temperatures as well as provide a tremendous weight reduction due to the reduced need for environmental control units in future Air Force weapon systems. This reduction in weight directly correlates into more fuel and weapons load for future aircraft, and the increased electronics reliability translates into higher mission capability.

Weight reduction, increased reliability, and radiation hardness also makes SiC an ideal candidate for space applications where the operating environment puts tough performance restrictions on electronic packages. Again, the elimination of the need for large environmental control units and burdensome heat radiators provides a liftoff weight reduction which has a major

impact on the mission. Furthermore, due to SiC's high resistance to radiation damage, the reduced need for heavy electronic shielding provides a further weight savings. Perhaps even more important for space missions is SiC's excellent physical stability, which equates to increased performance and reliability for long term missions in space.

1.2 High Power and High Frequency Devices

SiC's ability to operate at high power and high frequencies make it an ideal choice for high power microwave field effect transistors or MESFETs. Wright Laboratory in conjunction with Westinghouse Research Center in Pittsburgh, PA, is working to develop suitable SiC material for these devices. Recent efforts at Westinghouse have produced 6H-SiC MESFETs operating with a drain voltage of 50V with measured power levels of 1.8 W at 10 Ghz.[1] This power level is far from the predicted rf output powers of 65 W at 10 Ghz for 6H-SiC MESFETs.[2] Current MESFETs are limited by the conductivity of SiC substrates which is caused by residual impurities such as nitrogen, aluminum, and boron. The development of insulating or semi-insulating material is needed to improve these devices.

The introduction of deep level traps at mid-gap is necessary to compensate for nitrogen donor or boron acceptor impurities in SiC. Westinghouse is attempting to compensate the impurities with vanadium, a transition metal impurity in bulk SiC, which forms a deep donor state and an acceptor state in SiC's bandgap. Westinghouse's efforts are centered on intentionally doping SiC material with vanadium during the sublimation growth process. Doping with vanadium is difficult due to the low solubility of vanadium in SiC. The controllability of the dopant level and the dopant uniformity are two problems that must be solved to achieve adequate insulating or semi-insulating material. In an effort to solve these problems, Wright Laboratory is performing Optical Admittance Spectroscopy, temperature dependent Hall Effect, and Optical Absorption measurements in order to characterize the deep levels in SiC.[3]

1.3 Purpose of Research

The purpose of this work is to characterize, through low temperature photoluminescence spectroscopy, 4H- and 6H-SiC bulk material grown by the sublimation process at the Westinghouse Research Center. Photoluminescence provides a quick and nondestructive diagnostic technique for determining the nature and uniformity of polytype growth of SiC. Moreover, much can be learned about both the shallow and deep centers introduced, either purposely or by accident, during the growth process. Both intentionally vanadium doped and unintentionally vanadium doped p-type material from Westinghouse were studied to determine crystal quality and impurity identification. More importantly, the suitability of vanadium as a dopant to compensate for SiC's intrinsic conductivity was examined.

1.4 Thesis Organization

This thesis is divided into six chapters. The first chapter provides an explanation on why it is important to study SiC. Chapter two reviews the crystal structure and the sublimation growth of SiC. Chapter three provides an overview of photoluminescence principles and the experimental apparatus used to obtain the luminescence data. Next, chapter four examines the primary luminescence centers in SiC. Finally, chapters five and six presents and discusses the photoluminescence results from the Westinghouse samples studied in this work.

2. BACKGROUND

2.1 Crystal Structure of SiC

SiC belongs to a class of materials that exhibits a one-dimensional polymorphism called polytypism. SiC crystals consist of bilayers of Si and C bonded tetrahedrally and stacked upon each other. Different polytypes arise from different stacking arrangements of the bilayers. The nearest neighbors for different polytypes are the same; however, differences arise when the second and third nearest neighbor atoms are considered.[4]

Numerous possibilities exist for different sequences of stacking layers so a special nomenclature has been developed to identify the polytypes of SiC (see Table I). In the pure zincblende structure, there are three alternating bilayer pairs of Si and C, and the regular succession of the alternating bilayers are indicated by the letters ABCABC. In the pure wurtzite structure there are two alternating bilayer pairs, and the stacking sequence is ABAB. In all cases, the stacking sequence is along the c-axis. SiC exists in three basic forms indicated by the letters C (cubic), H (hexagonal), and R (rhombohedral). Thus, for the pure cubic structure shown in Figure 1 the notation 3C-SiC is given where the number 3 refers to the periodicity of the stacking layer and the letter C denotes the overall symmetry of the crystal. Likewise, the pure wurtzite configuration shown in Figure 2 is denoted by 2H-SiC where the overall crystal symmetry is hexagonal.

Table I: SiC Polytype Nomenclature[5]

Ramsdell Notation	ABC Notation	No. of inequivalent sites	No. of cubic sites	No. of hexagonal sites
2H(wurtzite)	**AB**	**1**	**0**	**1**
3C(zincblende)	**ABC**	**1**	**1**	**0**
4H	**ABAC**	**2**	**1**	**1**
6H	**ABCACB**	**3**	**2**	**1**
15R	**ABCACBCABACABCB**	**5**	**3**	**2**

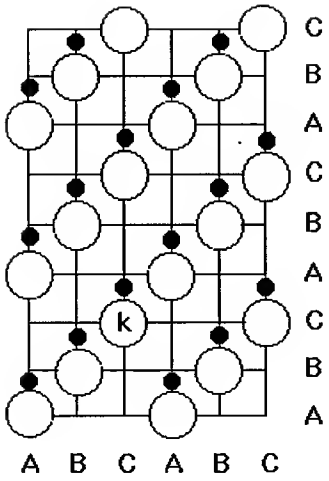

Figure 1: Crystal Structure of cubic 3C-SiC. Each lattice site, k for cubic symmetry, is equivalent.

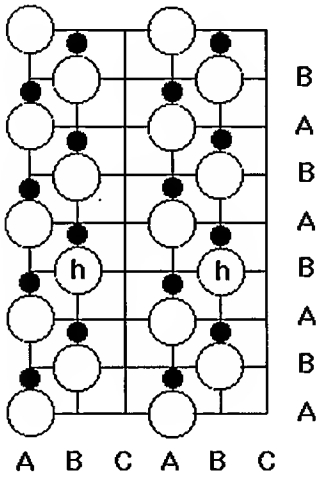

Figure 2: Crystal structure of hexagonal 2H-SiC. Each lattice site, h for hexagonal symmetry, is equivalent.

2H and 3C are the only pure symmetry polytypes of SiC. All other polytypes are a mixture of cubic and hexagonal bonding structures. The two most common hexagonal polytypes of interest here are 4H- and 6H-SiC (see Figure 3 and Figure 4). 4H-SiC is composed equally of one-hexagonal and one-cubic inequivalent site. The term inequivalent site is used to note the differences in second- and third- nearest neighbor configurations for each site. Hexagonal sites have a wurtzite configuration of second- and third-nearest neighbors; whereas, cubic sites have the zincblende configuration of second- and third-nearest neighbors. 6H-SiC, which is the most common polytype (see Figure 4), is composed of one-third hexagonal and two-thirds cubic sites, but, the overall crystal symmetry remains hexagonal. For 6H-SiC, the two cubic sites are also inequivalent, but one must look at the third nearest neighbors to see the difference. As one will see in chapter 4, the existence of these inequivalent sites provides for a complex luminescence spectrum.

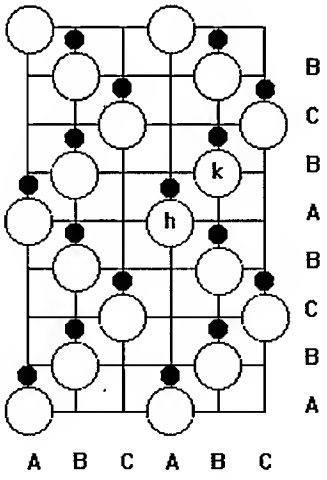

Figure 3: Crystal structure of 4H-SiC. Half the sites are hexagonal (h) and half are cubic (k).

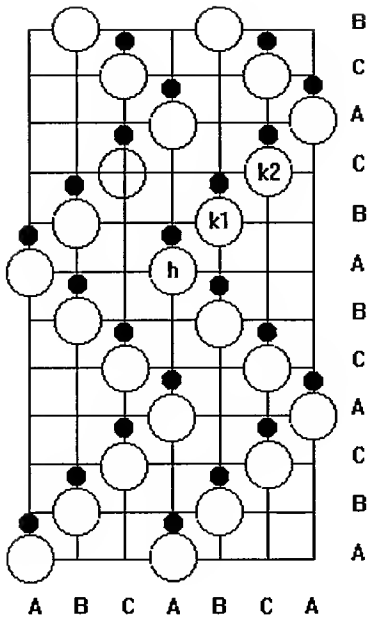

Figure 4: Crystal structure of 6H-SiC. One-third of the sites are hexagonal and two thirds are cubic. The cubic sites, k_1 and k_2 are also inequivalent.

2.2 SiC substrate crystal growth

SiC enjoys one major advantage over other wide-bandgap semiconductors like GaN, that is, there exists an established process for the growth of high-quality substrate material. The method of choice for the production of SiC substrate material is the sublimation method. The production of 1" wafers is standard and the production of 2" wafers is improving but such wafers are still not available in large quantities. Furthermore, these wafers can be grown either n- or p-type conductivity depending upon the dopants used.[1]

The sublimation method is characterized by the transport of SiC in the vapor phase through a temperature gradient to a SiC seed crystal. Figure 5 shows the schematic for Westinghouse's sublimation growth chamber. In their method, the growth occurs with the deposition of Si and C in the vapor phase upon an inverted SiC seed crystal. The vapor is created by sublimation of a SiC source charge contained in a graphite crucible heated to temperatures

greater than 2000°C. The apparatus is an induction heated system with the hot zone of the furnace made of high-purity graphite parts. The crystal growth proceeds in an ultra-high-purity argon ambient. A typical growth cycle, which can last for as long as seventeen hours, is shown in Figure **6** which indicates the changes in source and seed temperatures and the argon pressure with time.

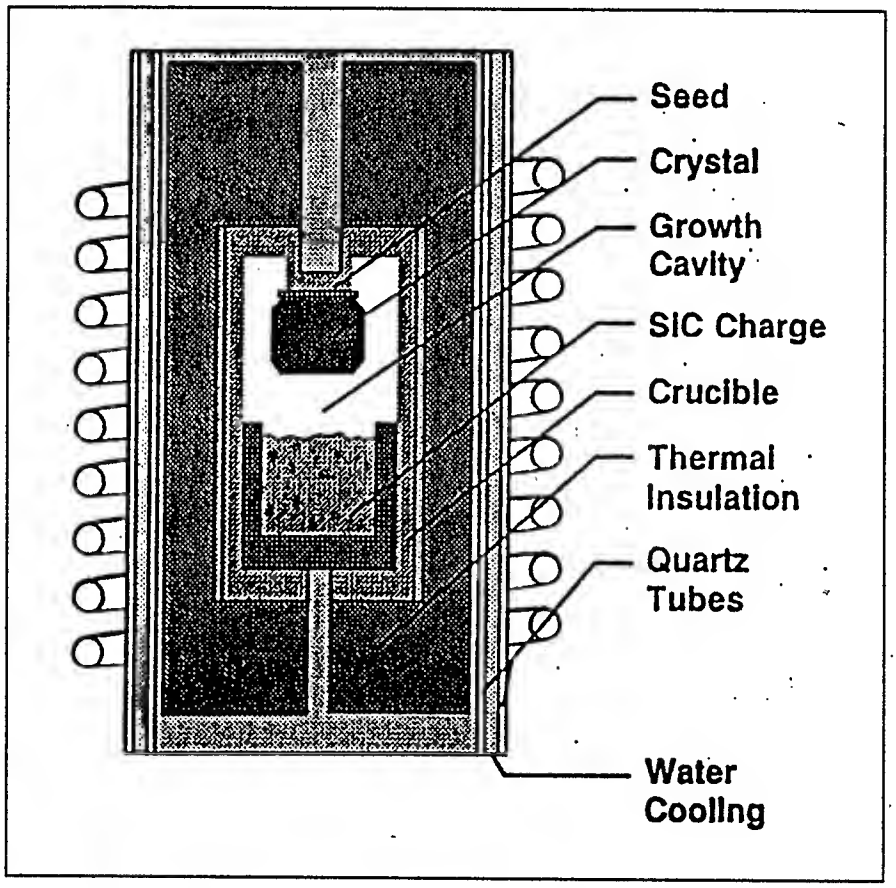

Figure 5: SiC sublimation growth apparatus.[6]

The total impurity content of the SiC crystals grown by the sublimation method depends strongly on the impurity content of the starting material, the quality of graphite parts, and the purity of the argon gas. Due to the high temperatures involved, >2000°C, almost all metallic elements (Ti, V, Cr, Ni, and Fe) act as contaminants due to their relatively high vapor pressures in the growth chamber. Thus, the structure of the furnace itself acts as a major source of

contaminants in SiC crystals. Contamination from the furnace is reduced by long bake out periods of the chamber and the use of high-quality graphite parts. Intentional doping of SiC grown by the sublimation method is typically achieved by mixing the dopant directly into the SiC source material. To achieve p-type conductivity, aluminum or boron is added to the source material, and to achieve n-type conductivity, it is necessary to instill a partial pressure of high-purity nitrogen gas into the growth chamber.

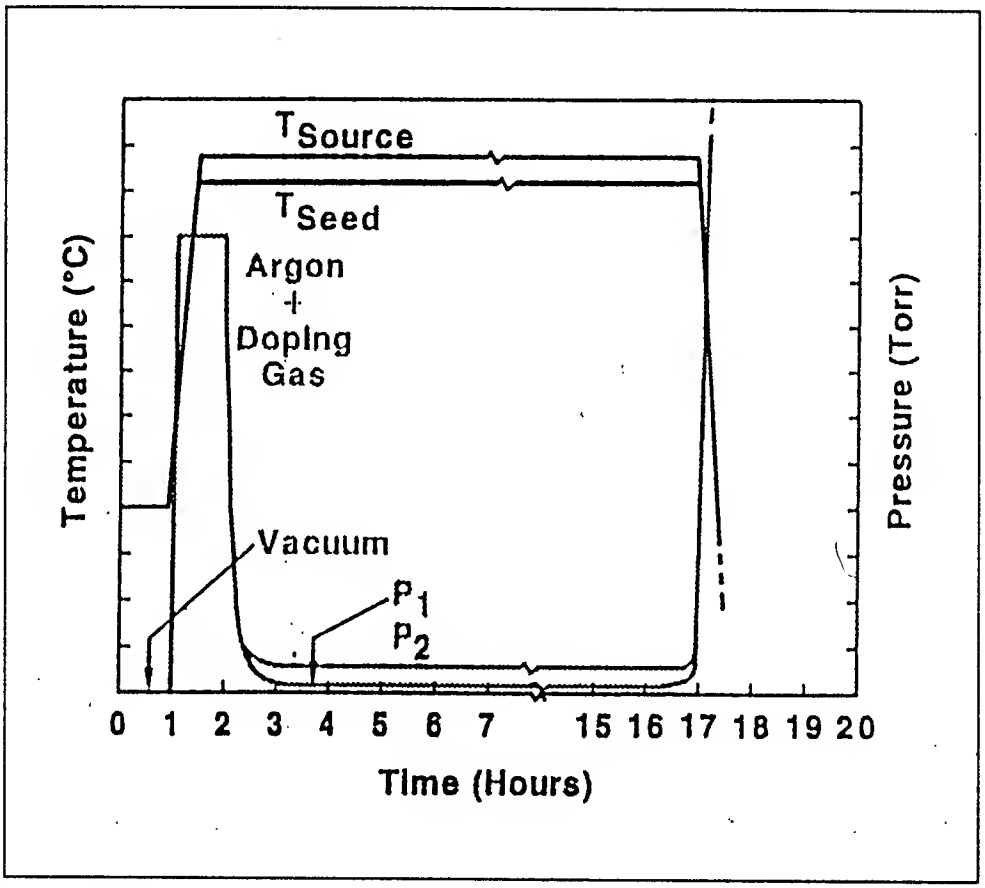

Figure 6: Typical growth sequence for SiC crystals grown by the sublimation method.[6]

Most 6H-SiC crystal grown by the sublimation method at Westinghouse are p-type with hole mobilities of 30 to 40 $cm^2/V\ s$.[6] The primary dopant responsible for the p-type conductivity in the Westinghouse material studied in this work is boron with a concentration of approximately 10^{16} to $10^{17}\ cm^{-3}$. This was determined by temperature dependent Hall measurements at

Westinghouse. These measurements showed an activation energy of approximately 0.35 eV, consistent with previously reported values for the ionization energy of boron in 6H-SiC. The source of the boron contamination is the carbon parts of the growth chamber. Boron is the primary contaminant in commercial high-purity graphite and has a vapor pressure greater than 10^{-4} atm. at the growth temperature.

2.3 Impurity Levels in SiC

A great deal of research has been performed on SiC in an attempt to determine the impurity levels in the bandgap. Figure 7 is an energy level diagram indicating the relative positions of each impurity level. The most studied impurities are the nitrogen donor and the aluminum acceptor. This is because nitrogen is the main dopant used to achieve n-type conductivity and aluminum is the main dopant used to achieve p-type conductivity. However, more acceptors are known to lie in the bandgap of SiC such as gallium, boron, and scandium which are indicated in the energy level diagram. Aluminum and boron are still the elements of choice to obtain p-type conductivity due to established doping procedures during growth.

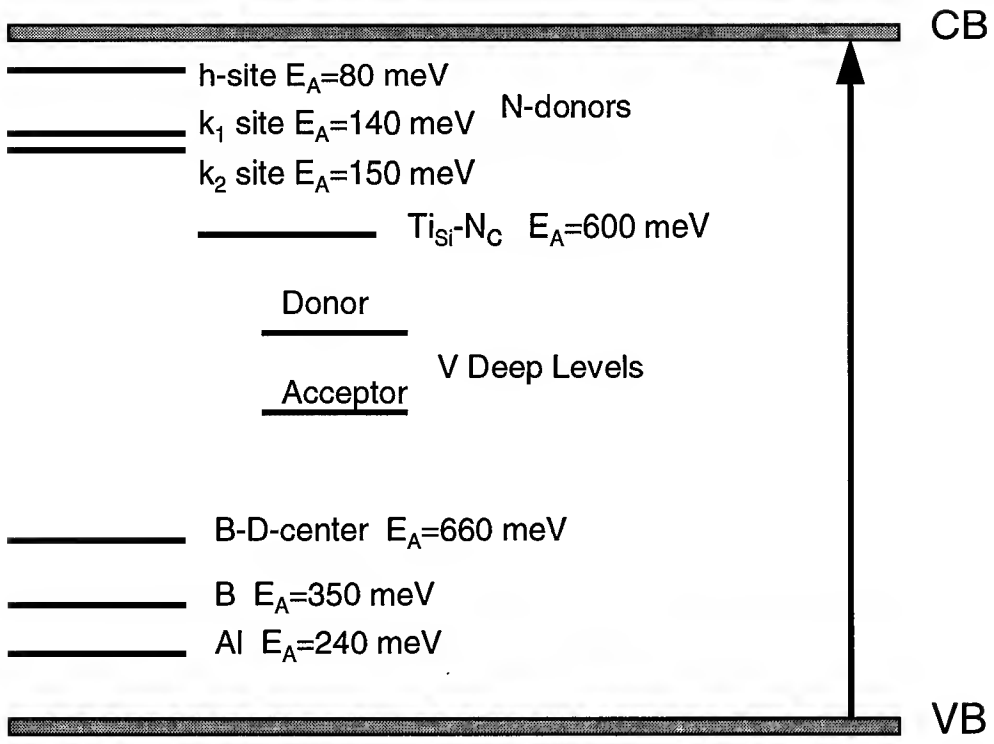

Figure 7: Energy level diagram for 6H-SiC. The activation energies shown are averaged due to variations in measurement techniques.

3. Equipment and Procedures

3.1 Introduction

This chapter provides an overview of photoluminescence and the equipment used to obtain luminescence data. Furthermore, a listing and discussion of the samples studied for this work is presented along with the sample number scheme.

3.2 Luminescence

When a semiconductor absorbs a photon of energy greater than the bandgap, an electron is excited from the valence band into the conduction band leaving behind a hole. The electron may return to its original state through radiative recombination or non-radiative recombination. When the electron recombines with the hole through radiative recombination it is called luminescence because a photon is emitted after recombination. Such transitions must conserve energy and momentum; thus, since SiC is an indirect bandgap semiconductor, the transition inside SiC requires the aid of a phonon to conserve momentum.

When impurities are present in the semiconductor, discrete energy levels exist in the forbidden gap. These energy levels are known as donor or acceptor levels. Donor levels are formed below the conduction band and acceptor levels are formed above the valence band. In addition, some impurities, like vanadium in SiC, may form levels in the middle of the gap and are called deep levels. All of these impurities act as recombination centers within the semiconductor and up to seven basic transitions are possible when an electron tries to recombine with a hole. By studying these transitions, clues to the nature of the impurities within the bandgap can be obtained.

3.3 Photoluminescence Apparatus

A schematic of the photoluminescence system is shown in Figure 8. The luminescence was generated by a Coherent Innova 300 Series Krypton Ion Laser operating on two ultraviolet lines at 3501 Å (3.54 eV) and 3564 Å (3.48 eV). The samples were mounted with rubber cement on the end of a copper sample holder which was immersed in liquid helium pumped below the lambda point to obtain temperatures below 4K. For temperatures above 4K, the sample was not immersed in the liquid helium and the temperature was controlled via a Lakeshore Cryotronics Model 82L temperature controller. The temperatures stated in this work are accurate within ±0.1K. With each temperature change, the temperature was allowed to stabilize for twenty minutes before an experiment was attempted.

The luminescence was collected and focused on the entrance slit of a 3/4 meter Czerny-Turner Spex 1702 spectrometer (dispersion 11Å/mm). For near ultraviolet and visible measurements, the spectrometer was equipped with a 5000 Å blazed grating with 1200 grooves/mm. For near-infrared luminescence, the spectrometer was equipped with a 12.5 μm blazed grating with 600 grooves/mm. Photon counting was used for signal acquisition in the 3700 Å-8000 Å range. A liquid N_2 cooled Thorn model 9558B, S2 photomultiplier tube powered at 1200 volts by a Stanford Research Instruments PS350 high voltage power supply was used for detection. The signal from the PMT was amplified by a Stanford Research Instruments SR455 DC-300MHz amplifier set to provide a 25× signal amplification. The amplified signal pulses were then counted using a Stanford Research Instruments SR400 gated photon counter. The signal from the counter was then sent to a dedicated PC, via an A/D converter, for processing. Labtech Notebook version 6.0 was the data acquisition software. Phase sensitive detection was used for signal acquisition in the near infrared. The laser beam was chopped and a

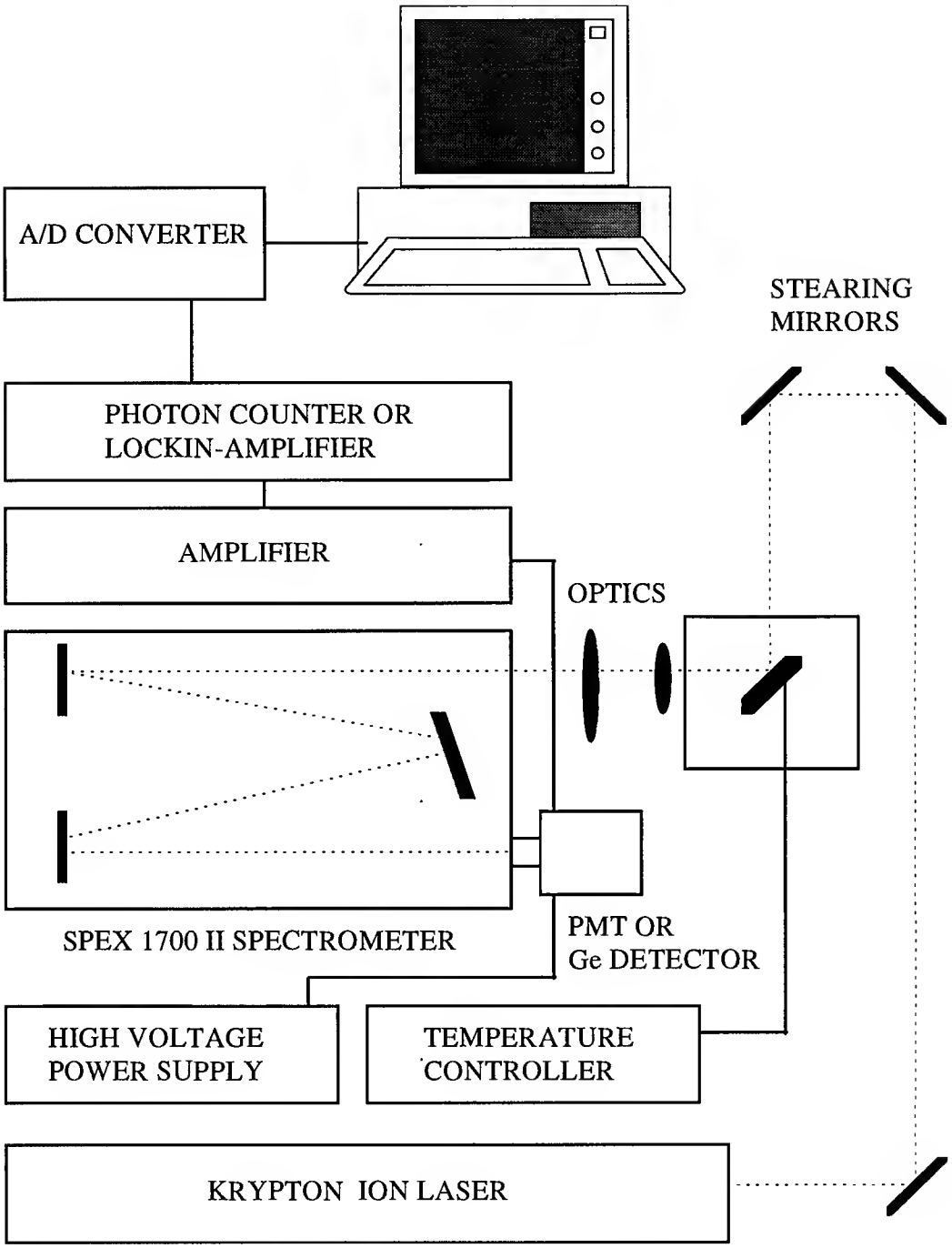

Figure 8: Photoluminescence Apparatus for Near UV and Near IR

cooled germanium detector with a Scitec Instruments 500MC lock-in amplifier was used for detection. This system was adequate for detection of signals from 8000 Å-15000 Å.

In both wavelength regions, the spectrometer was wavelength calibrated using an Oriel Kr lamp. A linear fit over the wavelength range of interest was obtained by matching known Kr lines from a scan of the lamp over the same wavelength range. This linear fit was used to correct the spectrometer dial reading to true wavelength during the data analysis in the Origin plotting software. A system response calibration was not performed because a blackbody source of high enough temperature, >2000°K, was not available. The high temperature was necessary to provide increased signal in the near UV for an adequate calibration. The system response is assumed linear, and the luminescence taken from SiC samples matches that found in published results which lends support to the linearity assumption.

3.4 Samples in the Study

All the samples studied in this work were provided by Dr. William Mitchel of Wright Laboratory Materials Directorate and are listed in Table II. Column 1 is the sample number and information in columns 2-6 includes grower, polytype, doping, growth method, and grower identification number. Samples from four separate growers were used in this study. Samples from Cree Research, Advanced Technology Materials (ATM) and the Ioffe Institute were used primarily to show the photoluminescence system was capable of reproducing the luminescence seen in published reports. The samples from Westinghouse were investigated for crystal quality, deep traps, and the attainment of vanadium doping.

Table II: Samples studied in this work. All Samples are Referenced with the AFIT ID Number.

Sample	Grower	Polytype	Doping	Growth Method	Grower ID
1	Cree	6H	N	Sublimation	B0436-4
2	Cree	6H	Al	Sublimation	E0104-3
3	Ioffe	6H	Undoped	Lely	23
4	Westinghouse	6H	Undoped	Sublimation	T-125-8
5	Westinghouse	6H	Undoped	Sublimation	T-127-3
6	Westinghouse	6H	Undoped	Sublimation	T-125-4
7	Westinghouse	6H	Undoped	Sublimation	K-30-17
8	Westinghouse	6H	V	Sublimation	K-32-14
9	ATM	6H	Undoped	Sublimation	9405SAF1-1
10	ATM	6H	Undoped	Sublimation	9311SAF1-2
11	ATM	6H	N	Sublimation	9405SAF1-2
12	ATM	6H	Undoped	Sublimation	D3073-5
13	Westinghouse	4H	N	Sublimation	T-151
14	Westinghouse	4H	Undoped	Sublimation	T-144-3
15	Westinghouse	6H	B	Sublimation	K-31-10
16	Westinghouse	4H	V	Sublimation	SN306-2
17	Westinghouse	6H	N	Sublimation	K-56-8
18	Westinghouse	6H	V	Sublimation	M8-14
19	ATM	4H	N	Sublimation	9408SAF1-1

4. Radiative Transitions in SiC

4.1 Introduction

The optical emission spectra of SiC is very complex because there are 12 atoms per unit cell, 6 C and 6 Si atoms, which results in 3N=36 branches in the phonon dispersion relation for 6H-SiC. Choyke and Patrick first studied the phonon spectrum of 6H-SiC with photoluminescence in 1962.[7] Table III shows the experimentally determined phonon energies they derived from their measurements. Figure 9 is a plot of the phonon dispersion relation from this data in extended **k** space. The extended **k** space is used only for convenience because the reduced zone representation is quite complex due to the large number of normal modes in the crystal.

Table III: The experimentally determined phonon energies for 6H-SiC. Energies are in meV.[7]

Phonon Branch	$k_c=0$	$k_c=2\pi/c$	$k_c=4\pi/c$	$k_c=6\pi/c$
TA	Forbidden	33.5, 36.3	39.2, 40.3	44.0, 46.3
LA	Forbidden	50.6, 53.5	67.0, 69.0	77.0
TO	98.8, 97.7	97.8	95.6	94.7
LO	120.3, 119.5	107.0	105.5	104.2

An additional reason for the complexity of the emission spectra was alluded to in chapter 2. The existence of inequivalent sites due to differences in second and third nearest-neighbor interactions results in site dependent ionization potentials for each impurity in SiC. Thus, multiple radiative transitions are seen for the same impurity atoms with their corresponding phonon series. To simplify things, this chapter provides an overview of the major luminescent centers in SiC which have been identified in published reports.

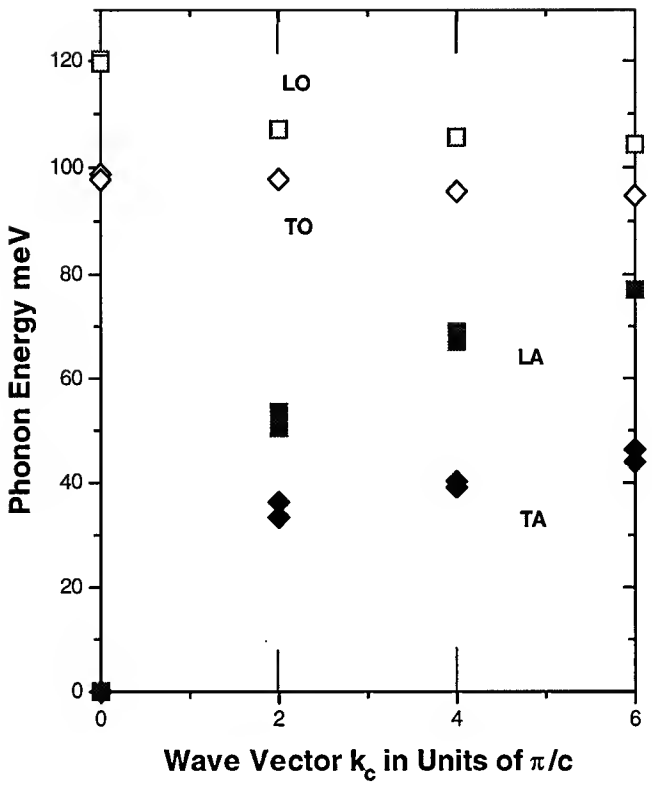

Figure 9: Phonon dispersion relation in extended **k** space for 6H-SiC.

4.2 Neutral Nitrogen Four Particle Lambert Complex

When an un-ionized donor captures an exciton, a four particle complex is formed. The complex consists of the donor ion and three electronic particles: two electrons and one hole. Recombination of the electron and hole within a four particle complex is what is meant by exciton recombination at an impurity atom. These four particle complexes are typically called Lambert complexes.[7]

Choyke and Patrick's initial photoluminescence investigations determined that the near band edge luminescence (3 eV to 2.9 eV) of 6H-SiC was attributed to an exciton bound to a neutral nitrogen donor. The connection with nitrogen was based on the intensity increase of the spectral lines with an increase in nitrogen concentration in the crystals studied. In addition,

studies of different polytypes have shown the near-band edge luminescence was due to bound exciton recombination at neutral nitrogen donors substituting for carbon in SiC.[7]

Figure 10 is a typical near band edge luminescence spectrum from a good quality bulk 6H-SiC crystal. The sample, grown by the sublimation process at Cree Research and intentionally doped with nitrogen, is n-type. The zero phonon lines (ZPLs), due to the neutral nitrogen bound exciton recombination, are marked P_0, R_0, and S_0. Exciton recombination in 6H-SiC requires an indirect transition; therefore, recombination without phonon emission is forbidden for *free* excitons. The binding of the exciton to the neutral nitrogen donor complex makes these ZPLs possible.

The P_0 peak has been attributed to the neutral nitrogen bound exciton at the hexagonal site. The R_0 and S_0 peaks are excitons bound to the neutral nitrogen complex at the two cubic sites k_1 and k_2. The binding energy of these excitons can be calculated from equation 1 where E_B

$$E_B = E_{GX} - h\nu - nh\omega \qquad (1)$$

is the exciton binding energy, E_{GX} is the excitonic band gap, $h\omega$ is the phonon energy and n is the number of emitted phonons. The excitonic bandgap is determined experimentally from absorption measurements or from the intrinsic (*free* exciton) photoluminescence spectrum, provided one phonon energy is known.[8] The accepted values of, E_{GX}=3.024eV for 6H-SiC, and, E_{GX}=3.265eV for 4H-SiC, are used in this work.[9] Table IV lists the energy position of the ZPLs and the binding energies of the neutral nitrogen bound excitons along with the known ionization energies for the nitrogen donors. The ionization energies were determined by infrared spectroscopic studies done elsewhere.[9]

Table IV: Exciton binding energies and nitrogen donor ionization energies for 6H-SiC.

Peak	Energy (eV)	Site	E_B (meV)	E_i (meV)
P_0	3.007	h	17	81.0
R_0	2.9924	k_1	31.6	137.6
S_0	2.9906	k_2	33.4	142.4

The complex phonon structure of 6H-SiC can also be seen in Figure 10. The lines marked P are phonons associated with the ZPL P_0. The subscripts indicate the phonon energy in meV of the line. As marked in the figure, all four branches of the phonon dispersion relation can be seen in this spectrum. In addition to the P_0 related phonons, the intrinsic phonon peaks can be seen. These lines are marked with the letter I, and their phonon energy is in subscripts. These peaks arise due to the recombination of *free* excitons which must have the aid of a momentum conserving phonon to make the transition and are known to occur only in high quality material. The energies of the intrinsic phonons are similar to those of the neutral nitrogen spectrum. Choyke and Patrick believe the presence of the nitrogen donor has little effect on the phonon energies; therefore, the phonon energies found in their experiments are believed to be lattice phonon energies.[7]

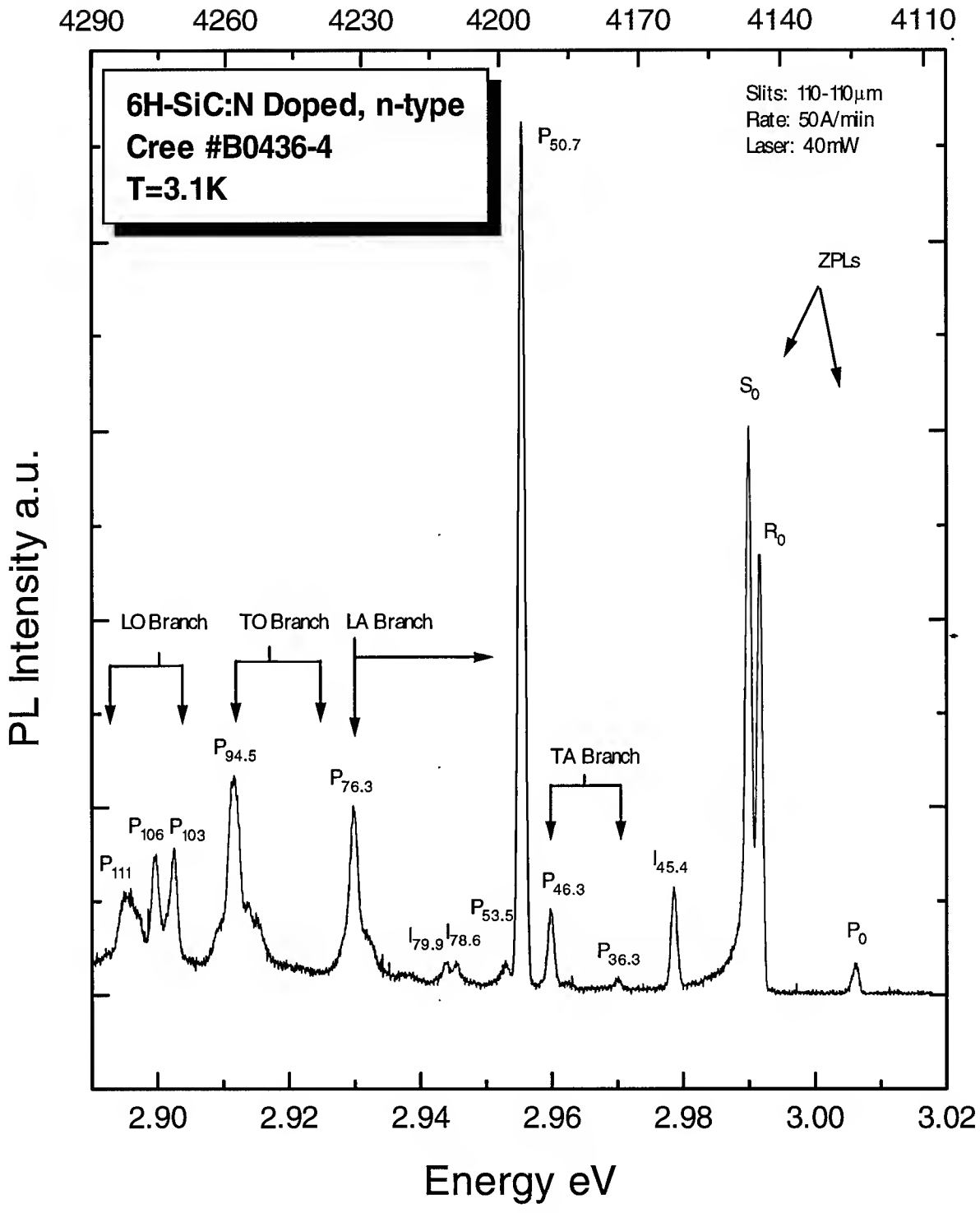

Figure 10: 6H-SiC:N doped, n-type near-band edge luminescence.

The near-band edge luminescence serves as a good indicator of the crystal quality. For example, Figure 11 is the near band edge luminescence from another 6H-SiC:N-doped, n-type sample which was grown by ATM using the sublimation process. The difference in line width can be attributed to the smaller slit width, 60 μm, used on the ATM sample compared to 110 μm for the Cree sample. Differences in crystal quality can be seen when one considers the absence of the intrinsic phonon spectrum in the ATM sample, as well as the absence of the 50.6 meV phonon peak which is very strong in the higher quality Cree sample. Typically, the presence of the intrinsic phonon spectrum is indicative of high quality material.

When the temperature is raised, the near band edge luminescence changes. Figure 12 shows three spectra taken at T=7.3K, 28.5K, and 45.0K. A new spectrum, which is a duplicate of the low temperature spectrum, appears displaced to a higher energy from R_0 and S_0. The duplicate of P_0 is not seen and is assumed to be lost in the background. The displacement of these lines are 4.8meV for R_{01} and 5.0 meV for S_{01}. These values are in good agreement with the 4.8±.3meV seen by Choyke and Patrick.[8] Choyke and Patrick suggested the origin of the excited states was due to the spin-orbit splitting of the valence band. Their model of the valence band is shown in Figure 13. The valence band is believed to be split into three bands with the smaller splitting of E_1 and E_2 , 4.8meV, due to spin-orbit interaction. The valence band is believed to be split even further into E_3 due to crystal field splitting of >30meV; however, no observable luminescence associated with this larger splitting is seen. The small 4.8meV splitting is equal, within experimental error, for each inequivalent site which supports the theory of spin-orbit splitting because the magnitude of the splitting would not be dependent on the ionization potential, unlike valley-orbit transitions which would depend strongly on the ionization potential.

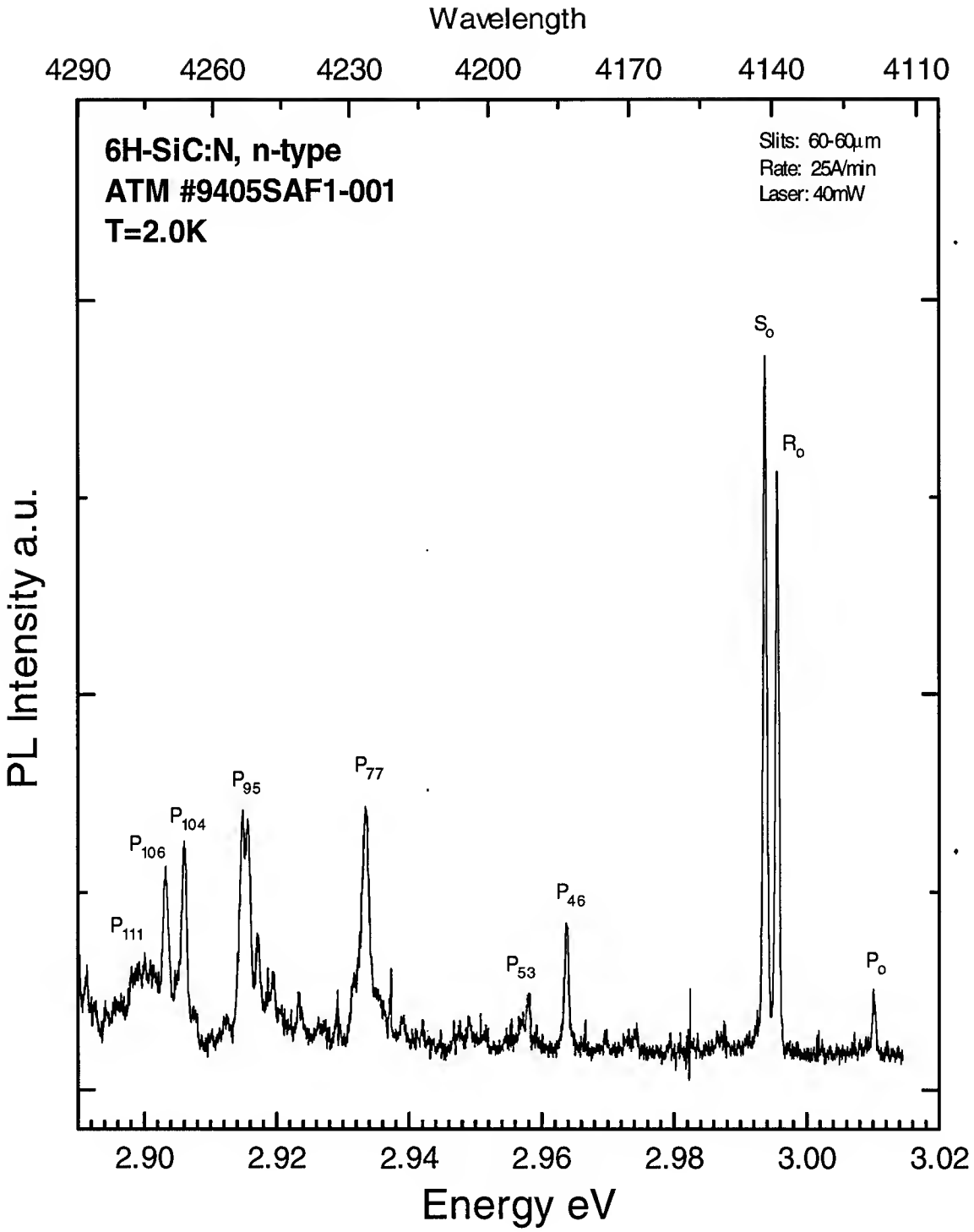

Figure 11: ATM 6H-SiC:N doped, n-type near-band edge luminescence. Note: The 50.6meV phonon along with the intrinsic phonons are absent indicating poorer quality material.

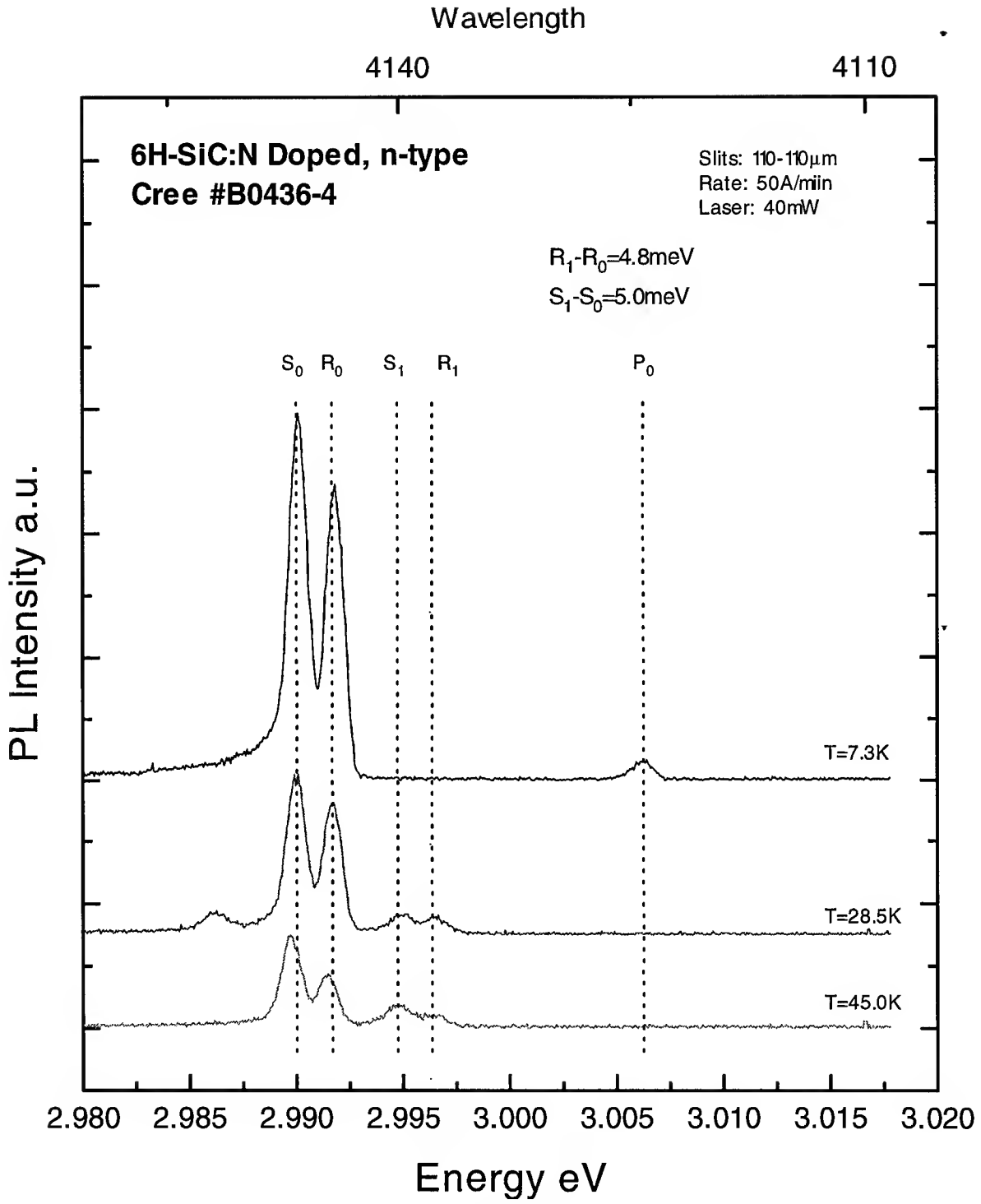

Figure 12: Temperature dependence of near band edge luminescence for 6H-SiC:N doped, n-type. The excited states are attributed to spin-orbit splitting of the valence band.

Figure 13: Valence band splitting of 6H-SiC as proposed by Choyke and Patrick.[8]

The near-band edge luminescence serves as a quick non-destructive technique for crystal polytype identification. The number of bound exciton peaks equals the number of inequivalent sites in the crystal. Unfortunately, in all the 4H-SiC samples studied in this work the nitrogen spectrum was quenched due to large amounts of other impurities in the crystals. However, the connection between the number of inequivalent sites and the number of exciton lines can be seen in the Ti bound exciton lines which is the subject of the next section.

4.3 Ti Bound Exciton Peaks

Further from the band edge, from 2.87 eV to 2.50 eV, another series of sharp line spectra appears in the SiC luminescence. Three ZPLs (for 6H-SiC) located at 2.862 eV, 2.821 eV, and 2.787 eV were first studied by Choyke and Patrick in 1963. They first suggested the lines were due to bound excitons at ionized nitrogen donors.[8] The assignment of these lines to bound excitons at ionized donors proved to be controversial. An investigation into the magneto-optical properties of these lines by Dean and Hartman (DH)[10] proved the lines were not due to excitons bound to ionized nitrogen donors. DH's argument centered on the problem of the large binding energy, >200 meV, of the excitons at ionized donors. They believed the large binding energy to

an ionized donor was in conflict with the exciton binding theory because the relevant effective electron-hole mass ratio is of order unity. Proof of the involvement of Ti in the low temperature luminescence was not confirmed, however, until 1974 by Kemenade and Hagen.[11] In this study, the intensity of the ZPLs increased with an increase in the doping of Ti. In addition, the doping with different isotopes of Ti produced several other ZPLs in the same energy region.

Ti is a group-IV element similar to Si and C; thus, it can be an isoelectronic trap in SiC. In a model proposed by Choyke and Patrick, they suggested that Ti($3d^0$) substituting for Si binds excitons. They believe, before recombination, the electron is trapped in the $3d_e$-orbital forming a localized A^--state Ti($3d^1$).[12] Furthermore, it will be shown that the Ti isoelectronic trap is tied to the valence band because in all polytypes the Ti luminescence occurs around 2.80 eV. To support this, one notes that the Ti luminescence is not present in 3C-SiC which has a bandgap energy less than 2.80 eV. Besides the luminescence work, little is known about the electrical activity associated with the Ti impurity in SiC. This lack of knowledge extends to vanadium, another transition metal impurity in SiC, which will be discussed later in this chapter.

Figure 14 and Figure 15 are the low temperature photoluminescence spectra of Ti impurities in 6H-SiC and 4H-SiC. The ZPLs marked A_0, B_0, and C_0 arise from exciton recombination at $Ti^{4+}_{Si}(3d^1)$. The lines marked A_{90}, B_{90}, and C_{90} are local phonon (≈90 meV) sidebands. B_{90} in the 6H-SiC spectrum is assumed lost in the background. The samples used for these spectra were grown at Westinghouse and are undoped, p-type samples. The crystals are p-type due to heavy Boron contamination. The exact location of the lines are given in Table V.

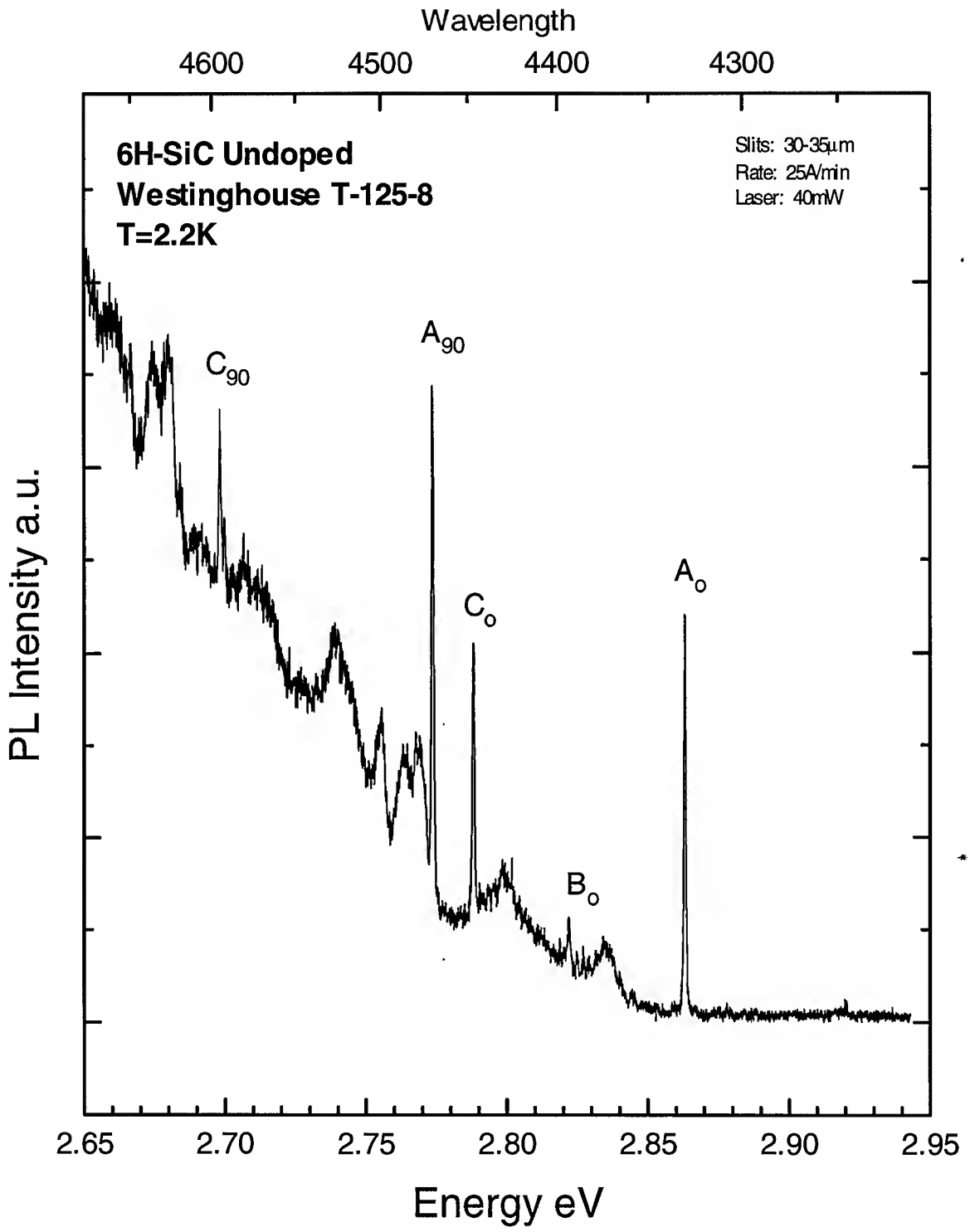

Figure 14: Ti bound exciton luminescence for 6H-SiC. Shown are the ZPLs and the 90 meV local phonon sidebands. A_0 and C_0 are assigned to cubic sites and B_0 is assigned to the hexagonal site.

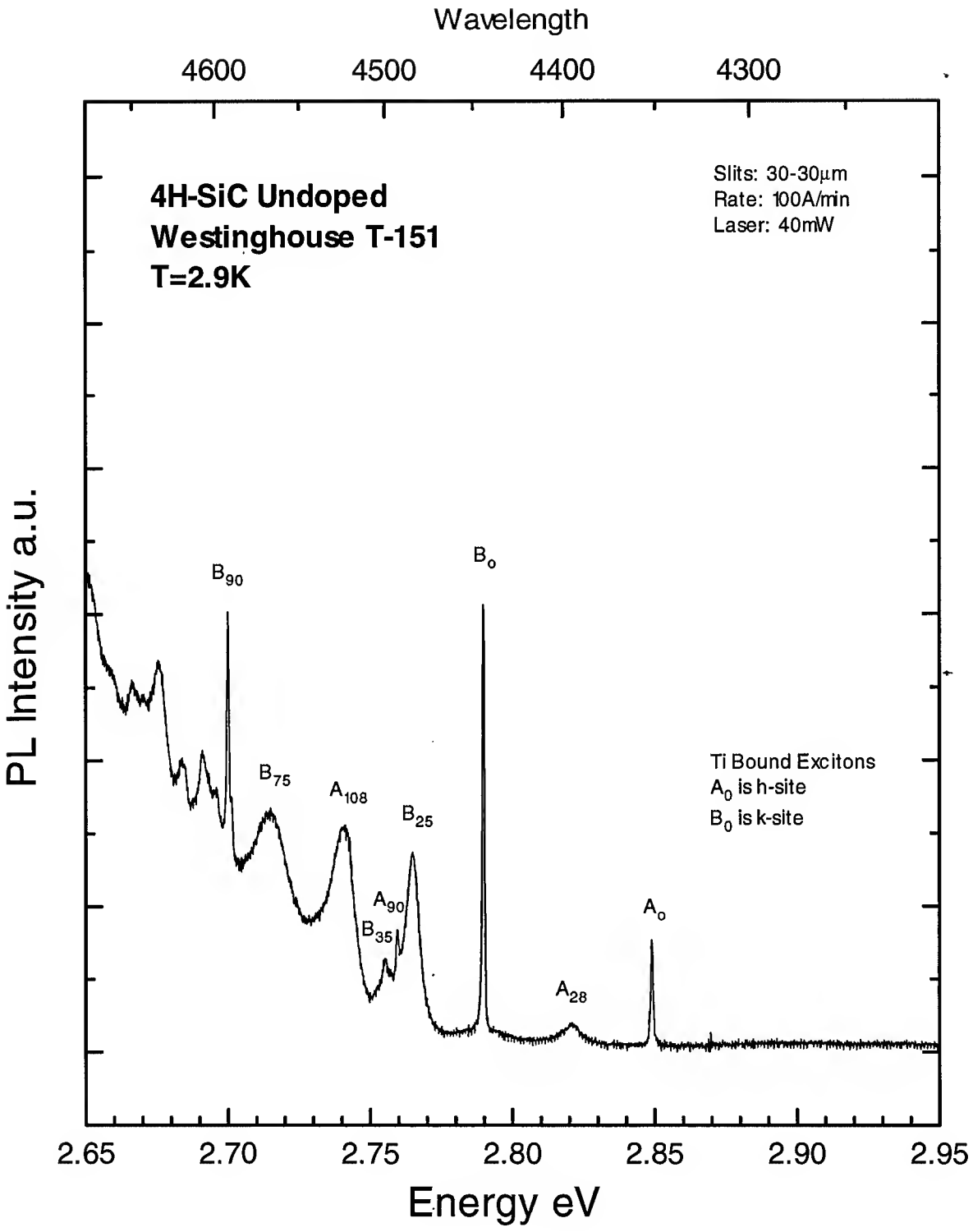

Figure 15: Ti bound exciton luminescence for 4H-SiC. Subscripts indicate phonon energy in meV from the noted line. A_0 is assigned to the hexagonal site and B_0 is assigned to the cubic site.

Table V: Ti bound exciton lines and 90meV local phonons for 4H-and 6H-SiC. Units are in eV.

Polytype	A_0	B_0	C_0	A_{90}	B_{90}	C_{90}
4H	2.849	2.790		2.760	2.700	
6H	2.862	2.821	2.787	2.773	2.732	2.698

Figure 16 and Figure 17 show the spectra of the same samples over a larger energy range. These spectra show the broad phonon luminescence peak arising from the Ti centers at ≈2.50 eV for 6H-SiC and ≈2.45 eV for 4H-SiC. The large Ti content was only observed in the Westinghouse samples. The spectrum from a nitrogen doped Cree sample in Figure 18 clearly shows less Ti contribution to the luminescence unlike the Westinghouse samples.

In Figure 14 and Figure 15, the number of ZPLs corresponds to the number of inequivalent sites in the crystal lattice. The site identification of the ZPLs is still under debate for 6H-SiC, but for 4H-SiC it is agreed that the A_0 line is at the h-site and the deeper B_0 line is on the k-site. For 6H-SiC, the h-site is believed to be associated with B_0 and the two cubic sites k_1 and k_2 are tentatively linked with A_0 and C_0.[10]

In Figure 16 and Figure 17 no nitrogen spectrum is seen in either Westinghouse sample. One explanation for the nitrogen spectrum being quenched was proposed by Choyke and Patrick.[8] They stated that with an increase in total impurity content an effect similar to impurity band hopping occurs. With increasing impurity concentration, the excitons on the shallower neutral nitrogen donors overlap and hop to deeper centers like Ti isoelectronic traps. Thus, the neutral nitrogen spectrum is quenched.

With an increase in temperature, thermally excited states of Ti bound excitons appear. Figure 19 is the temperature dependent spectra of a 4H-SiC Westinghouse sample. As the temperature is increased multiple lines on the higher energy side of A_0 and B_0 appear. The first

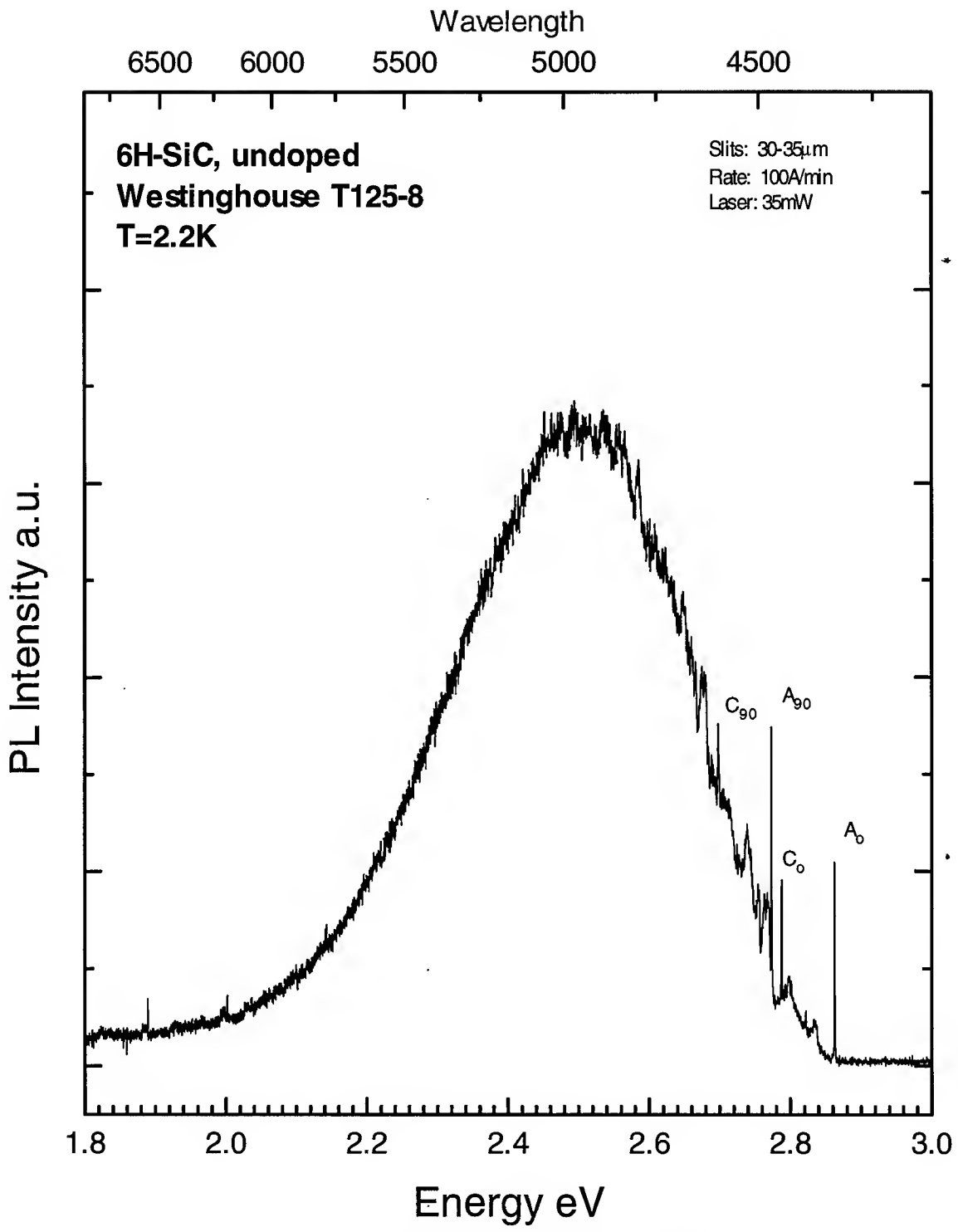

Figure 16: 6H-SiC sample showing the broad peak centered at 2.50eV due to many phonons of the Ti bound excitons.

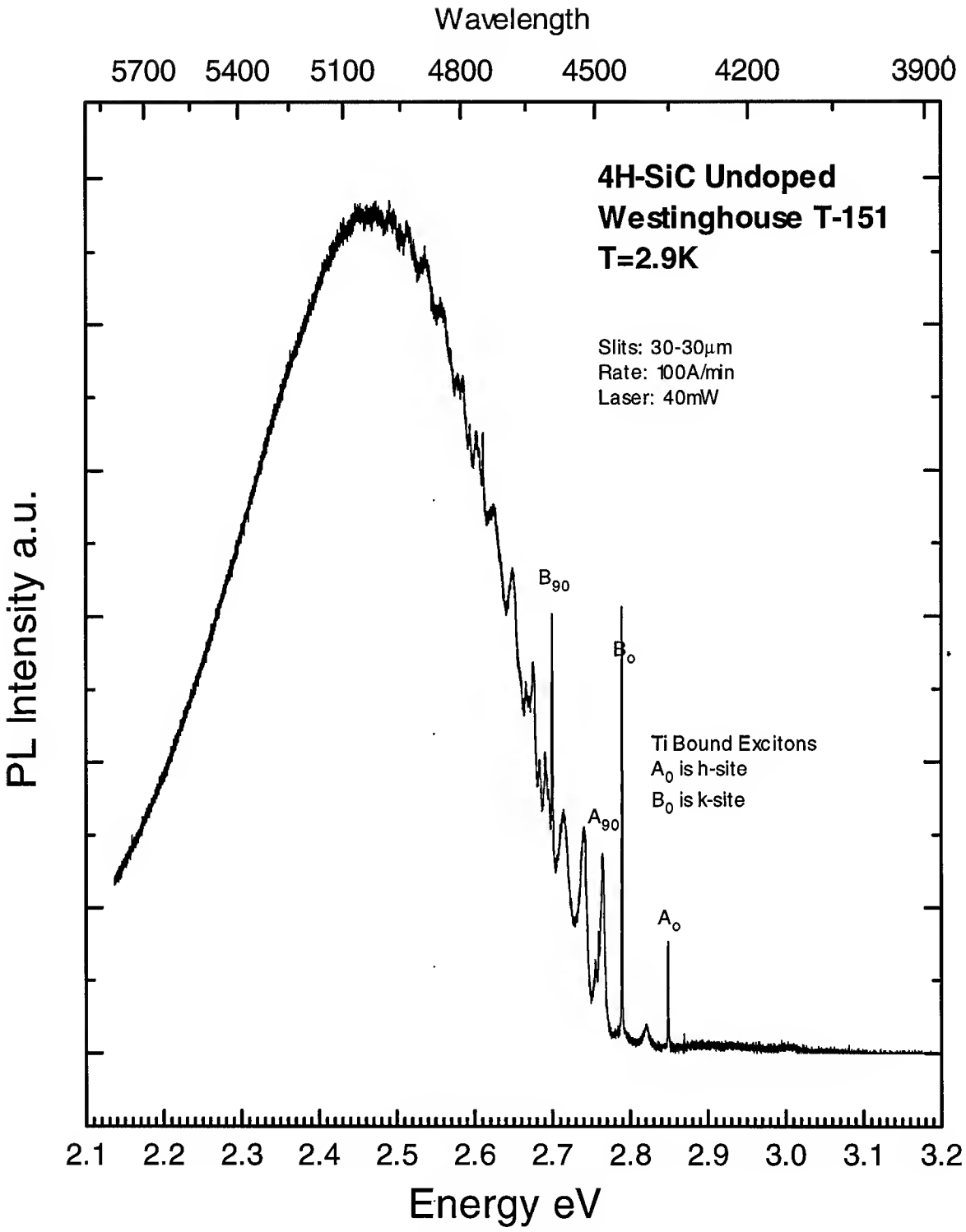

Figure 17: 4H-SiC sample showing the broad peak centered at 2.45eV due to many phonons of the Ti bound excitons.

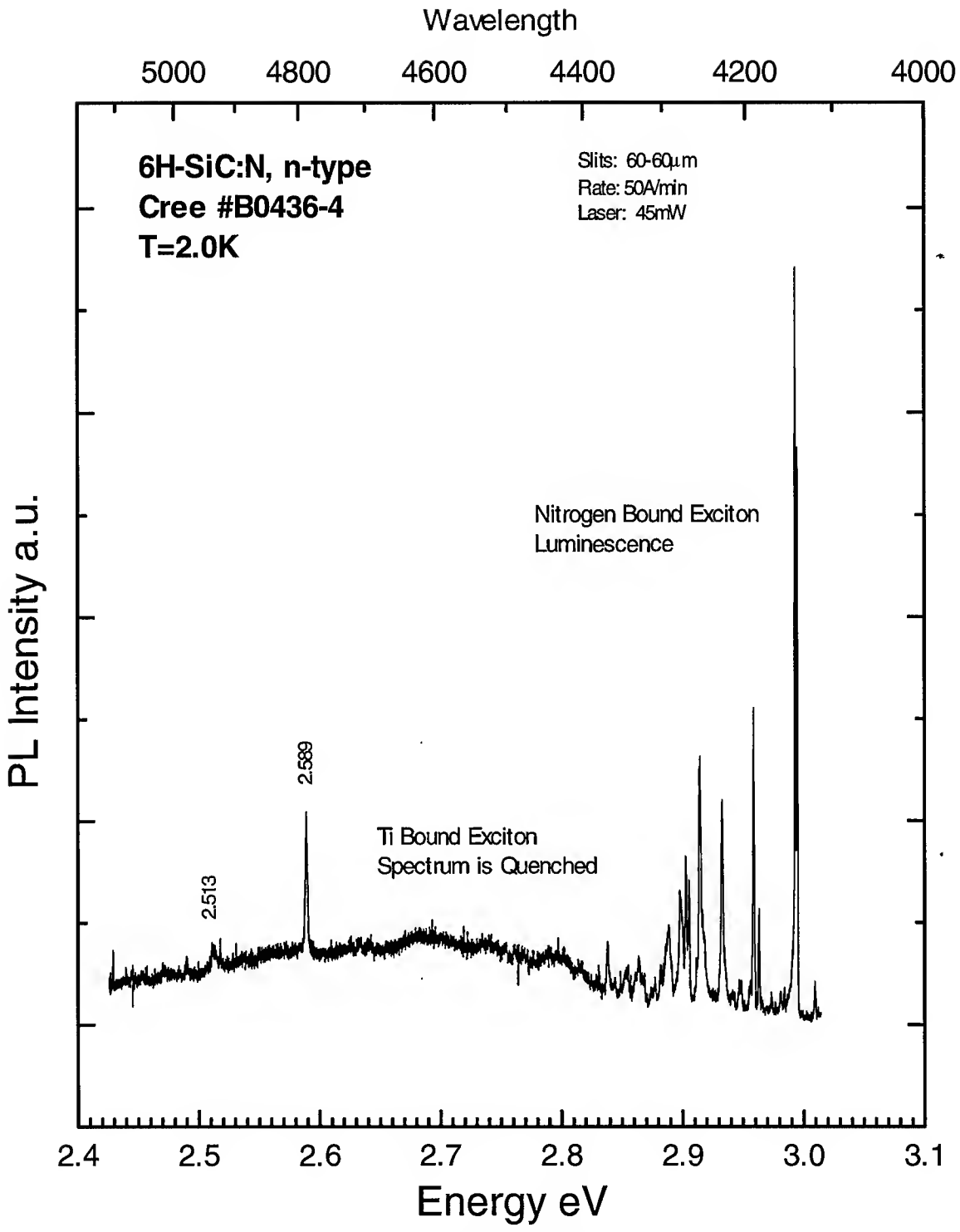

Figure 18: Luminescence from a Cree 6H-SiC sample. Note that the broad peak at 2.50eV seen in the Westinghouse samples is not present. In fact, the Ti bound exciton lines are quenched in this sample.

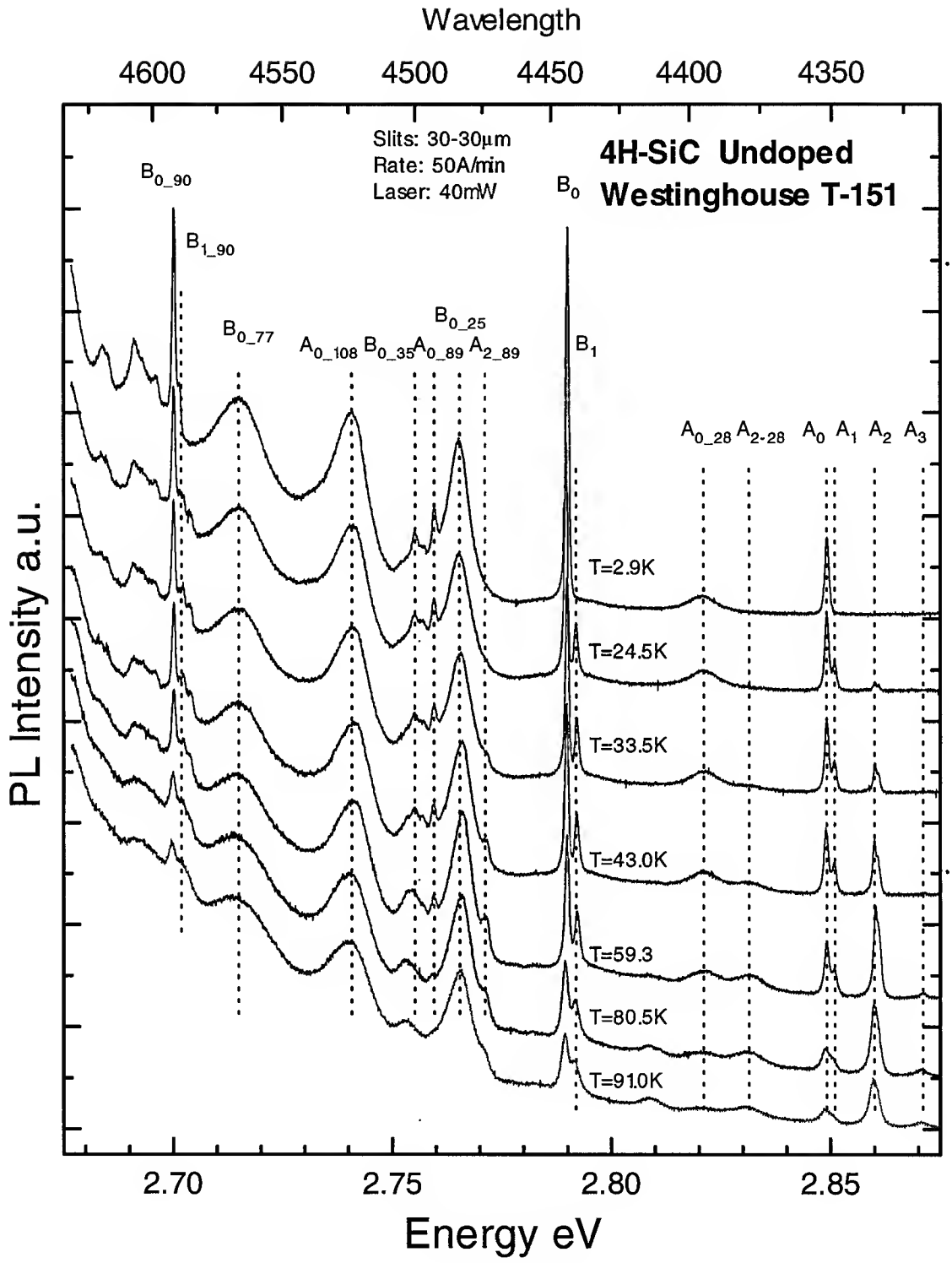

Figure 19: Ti bound exciton luminescence from 4H-SiC at various sample temperatures. The first subscript number indicates the state the line represents with 0 for ground state and all others are thermally excited states. The second subscript number indicates the phonon energy in meV of the line. The absence of a second subscript indicates a ZPL.

excited states, labeled A_1 and B_1, appear at about 15.0K. The energy separation from A_0 and B_0, respectively, is ≈2.0 meV for both sites and is repeated for the 90 meV local phonon B_{90} marked B_{1_90}. The 90 meV local phonon for A_1 is lost in the background. The second excited state A_2 appears at 24.0 K. A_2 appears to be a doublet and is 11 meV from A_0. The associated A_2 series includes 28meV and 90 meV phonon replicas which do not correspond to any known lattice phonons and are considered local phonons. At still higher temperatures, a third excited state, A_3, appears 22 meV from the ground state A_0.

The Ti spectrum is still strong at T=100 K which is far above any temperature that the nitrogen spectrum is observed. In addition, there is no luminescence from the 4.8 meV spin-orbit splitting as seen in the neutral nitrogen spectrum. The origin of the excited states in the Ti spectrum are attributed to valley-orbit transitions.[8] The multiple conduction-band minima of SiC are not at zero wave vector, and the 1*s* hydrogenic donor level splits due to valley-orbit coupling among states associated with the various conduction-band minima. Transitions among these level are called valley-orbit transitions which are populated at higher temperatures.[13]

4.4 N-Al Donor Acceptor Pair (DAP) Luminescence

6H-SiC crystals doped with Al acceptors and N donors emit bright blue luminescence due to donor acceptor pair (DAP) transitions.[14] The spectra is composed of two series of peaks denoted B and C. Figure 20 is the low temperature luminescence from a 6H-SiC:Al-doped Cree sample and Figure 21 is the low temperature luminescence from an undoped 4H-SiC ATM sample. Ikeda and Matsunami determined the B series was attributed to DAP recombination at hexagonal sites and the C series was attributed to DAP recombination at cubic sites.[15] They

suggested the relative heights of B_0 to C_0 gives information on site assignment. For 6H-SiC there is one hexagonal site and two cubic sites. Thus, assuming equal probability for transition between each site at low temperature and high excitation energy, the intensity of the DAP luminescence at cubic sites would be twice the intensity at hexagonal sites for 6H-SiC. From Figure 20 it was determined the intensity ratio of C_0 to B_0 was 1.9/1.0,measured with Origin plotting software, which agrees with Ikeda's findings. One would then expect the intensity of B_0 and C_0 to be equal in 4H-SiC which is the case in Figure 21.[16]

The phonon replicas shown in the spectra can be explained by assuming phonons common to all polytypes. The energies of the phonons are $E_{TA}\approx28$ meV, $E_{LA}\approx68$ meV, $E_{TO}\approx95$ meV, and $E_{LO}\approx107$ and ≈118 meV. The subscripts in Figure 20 and Figure 21 indicate the type of phonon with the associated series letter. The LA and TO phonons seen in the 4H are either too weak or are not present in the 6H spectrum.

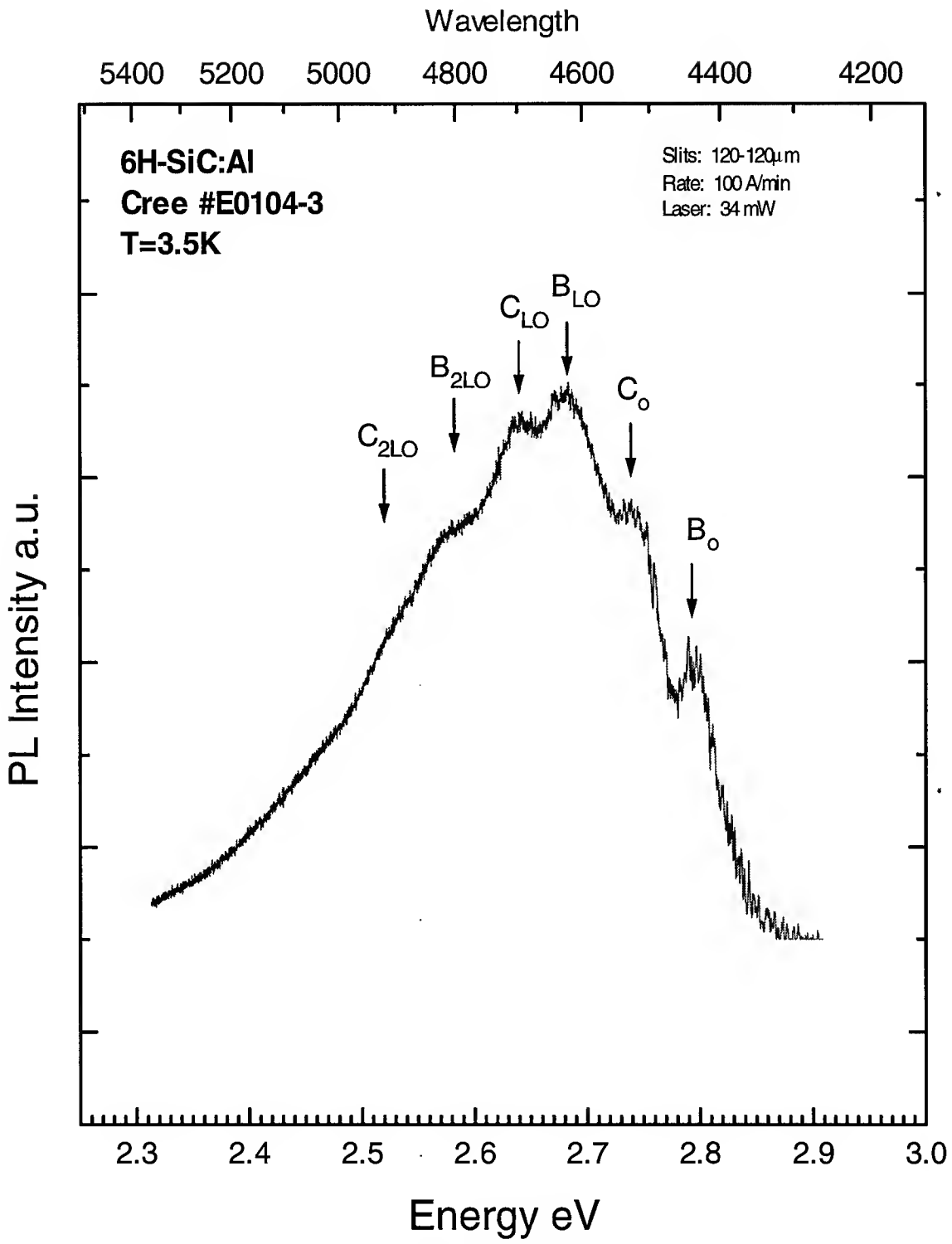

Figure 20: Photoluminescence spectra of Al doped 6H-SiC at 3.9 K. Subscripts indicate the kinds of phonons with $E_{LO} \approx 107$ meV.

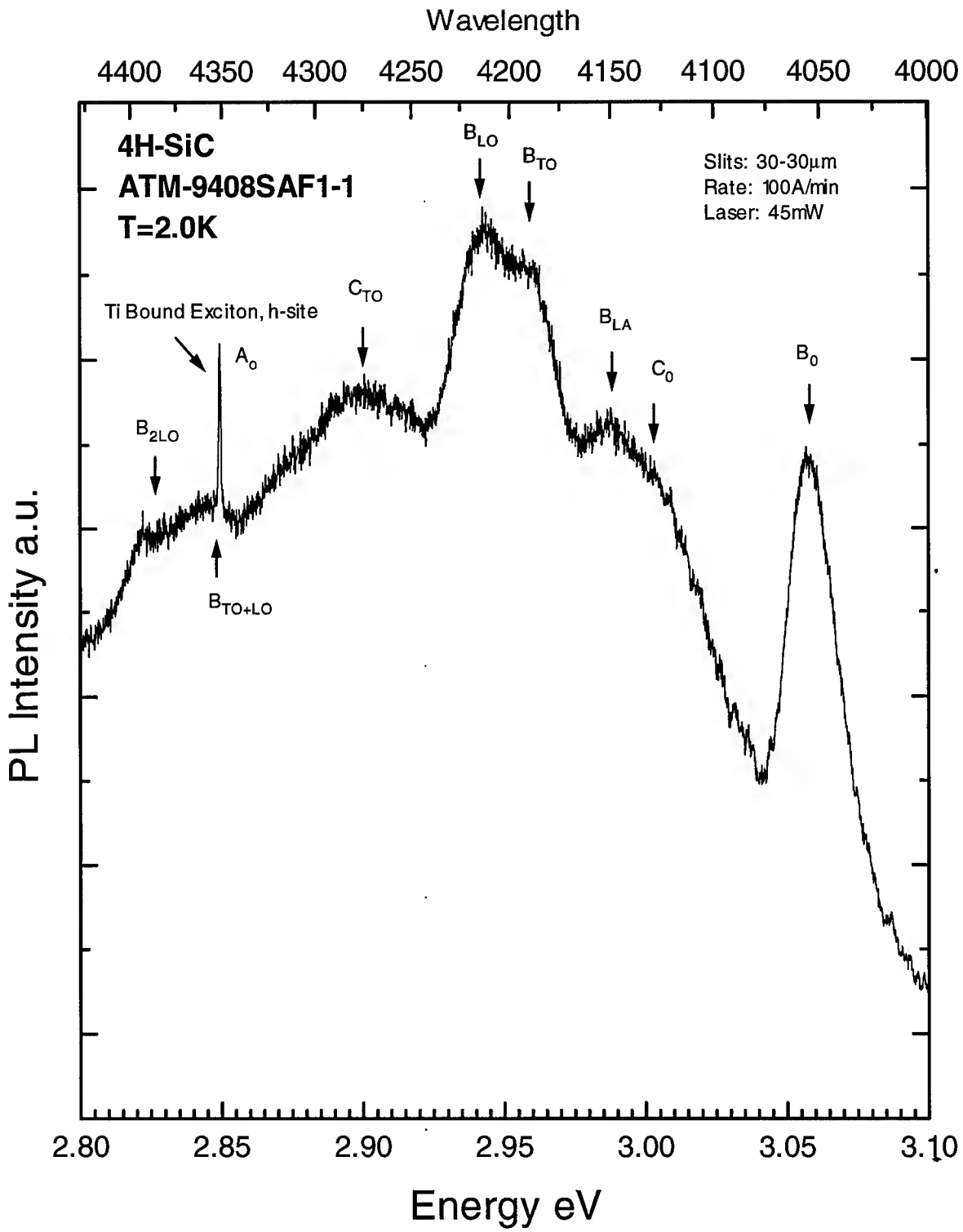

Figure 21: Photoluminescence spectra of an Al-doped 4H-SiC sample. Subscripts indicate the kinds of phonons with $E_{LA}\approx 68$ meV, $E_{TO}\approx 95$ meV, and $E_{LO}\approx 107$ meV.

The DAP luminescence shows a strong temperature dependence. Figure 22 is the spectra from the same Al doped Cree Research sample in Figure 20 but at T=90 K. The B series has been completely quenched at this temperature mainly because the electrons on the nitrogen donors occupying hexagonal sites have been thermalized at this temperature and are not available for DAP recombination. Not seen in Figure 22 is the free to acceptor peaks that appear at still higher temperatures. These peaks lie on the high energy side of B_0 at ≈2.9 eV. The free to acceptor peaks are typically labeled A_0^a and A_0^b with A_0^a attributed to free to acceptor recombination at hexagonal sites and the A_0^b peak attributed to free to acceptor recombination at the deeper cubic sites.[16]

The DAP luminescence also shows an acceptor concentration dependence. When a sample is strongly p-type, the Fermi level is near the acceptor level, and the ratio of the numbers of occupied donors in different sites is

$$N^H/N^C \cong \frac{1}{2}\exp\left[-\left(E^C - E^H\right)/kT\right] << 1 \qquad (2)$$

assuming a Boltzmann distribution where N^H and N^C are the numbers of donors in hexagonal and cubic sites.[16] Thus, from equation 2 the transitions due to donors in h-sites are far fewer than in k-sites and the B series is quenched at low temperature in strong p-type material. Figure 23 shows the low temperature luminescence from a 6H-SiC ATM sample. This sample is supposedly undoped; however, the luminescence suggests considerable aluminum content due to the absence of the B series at low temperature.

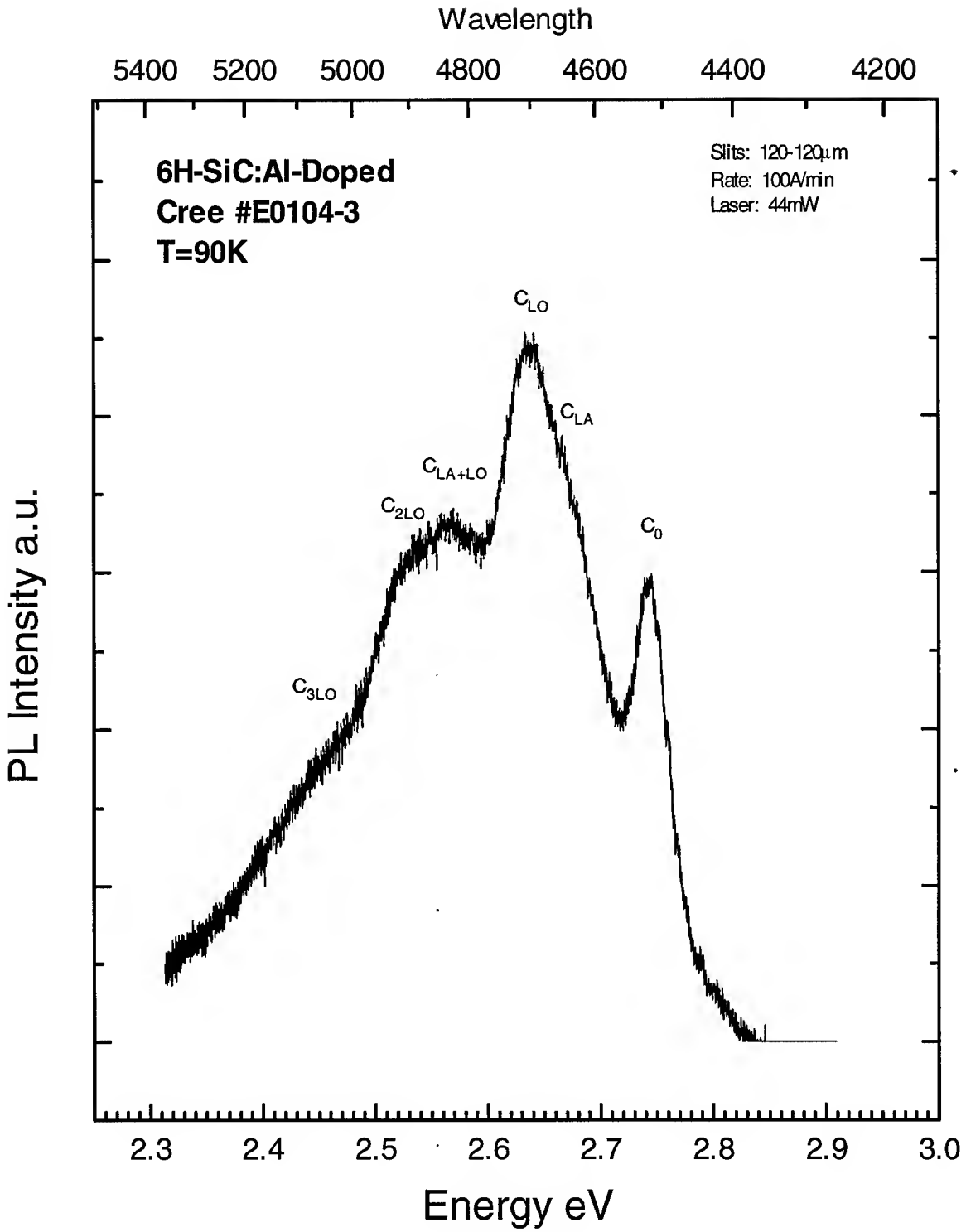

Figure 22: Photoluminescence spectra of Al-doped 6H-SiC at T=90 K. Subscripts indicate the kinds of phonons with $E_{LA} \approx 68$ meV and $E_{LO} \approx 107$ meV.

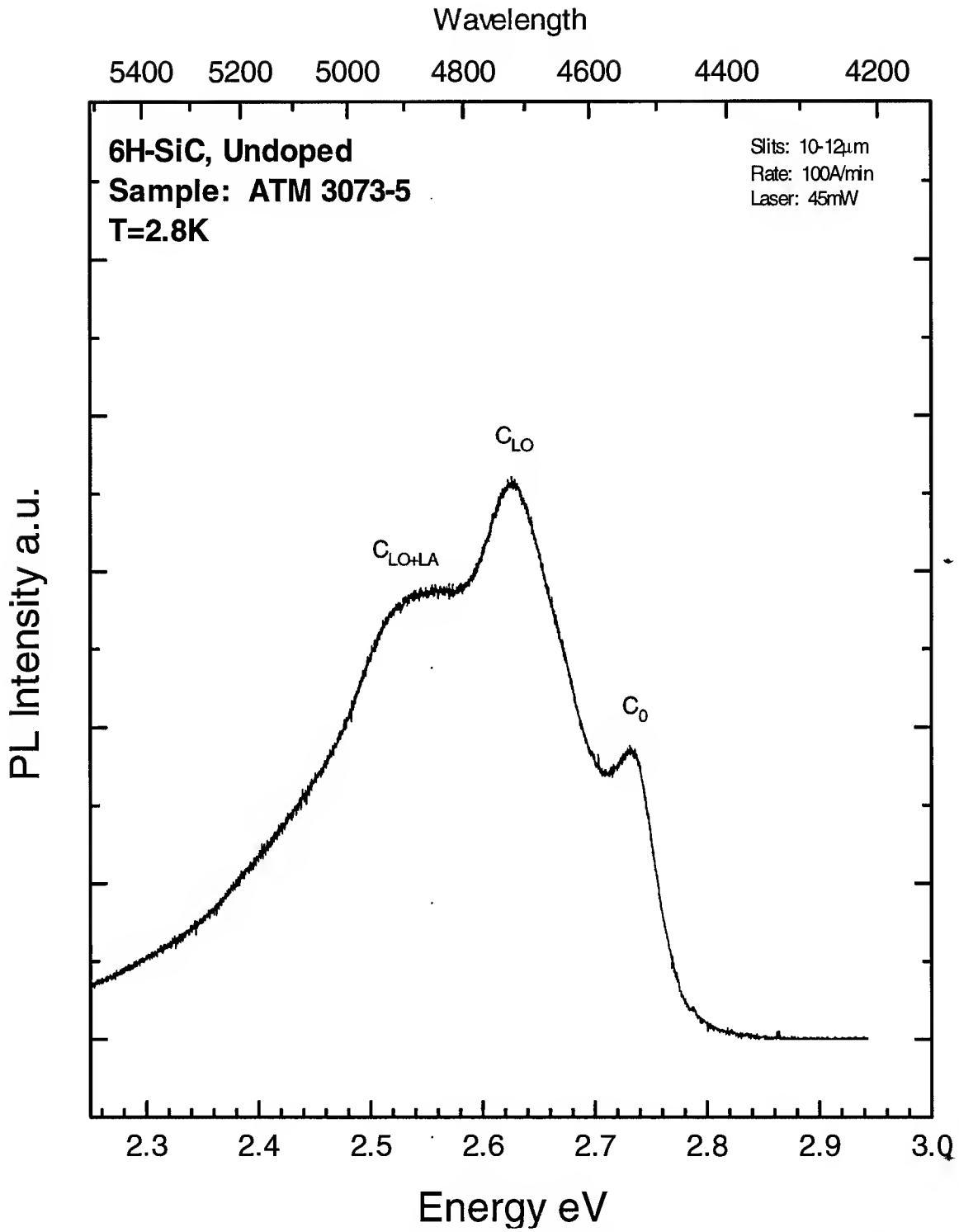

Figure 23: Low temperature photoluminescence spectrum from an undoped 6H-SiC sample. The luminescence was very strong, thus, a slit width of only 10 μm was used. The spectrum indicates substantial Al-doping in the crystal with the B series completely quenched at low temperature.

4.5 Aluminum Acceptor Four Particle Bound Exciton Complex

The production of high purity films with low nitrogen doping has allowed the detailed study of aluminum acceptors in lightly doped p-type SiC. The identification of a neutral aluminum acceptor, four particle bound exciton complex (4A) was made by Clemens and others in 1993.[17] The 4A complex is seen only in high purity single crystal films of 6H, 4H, and 3C-SiC lightly doped with aluminum. Thus, the data presented in this section is from the original work in 1993.

Figure 24 is the low temperature photoluminescence spectra of 6H and 4H-SiC thin films. Three spectra are shown for the 6H and two for the 4H polytypes. The top two spectra in Figure 24 are from undoped samples while the other spectra are from samples intentionally doped with aluminum. The shaded lines are the no-phonon lines of the 4A complex. The connection with aluminum is based on the increase in the 4A luminescence with an increase in the aluminum dopant levels. In both polytypes, the 4A complex appears between the P_0 and R_0 ZPLs which are from the neutral nitrogen bound exciton complex. In the case of 6H-SiC:Al, the lines are located between 3.0050 and 2.9996 eV. The binding energy of the 4A complex is estimated to be between 18-23.4 meV for 6H-SiC. Up to fifteen no-phonon lines have been seen in 6H-SiC to date and more are expected with improved crystal quality and higher resolution measurements.

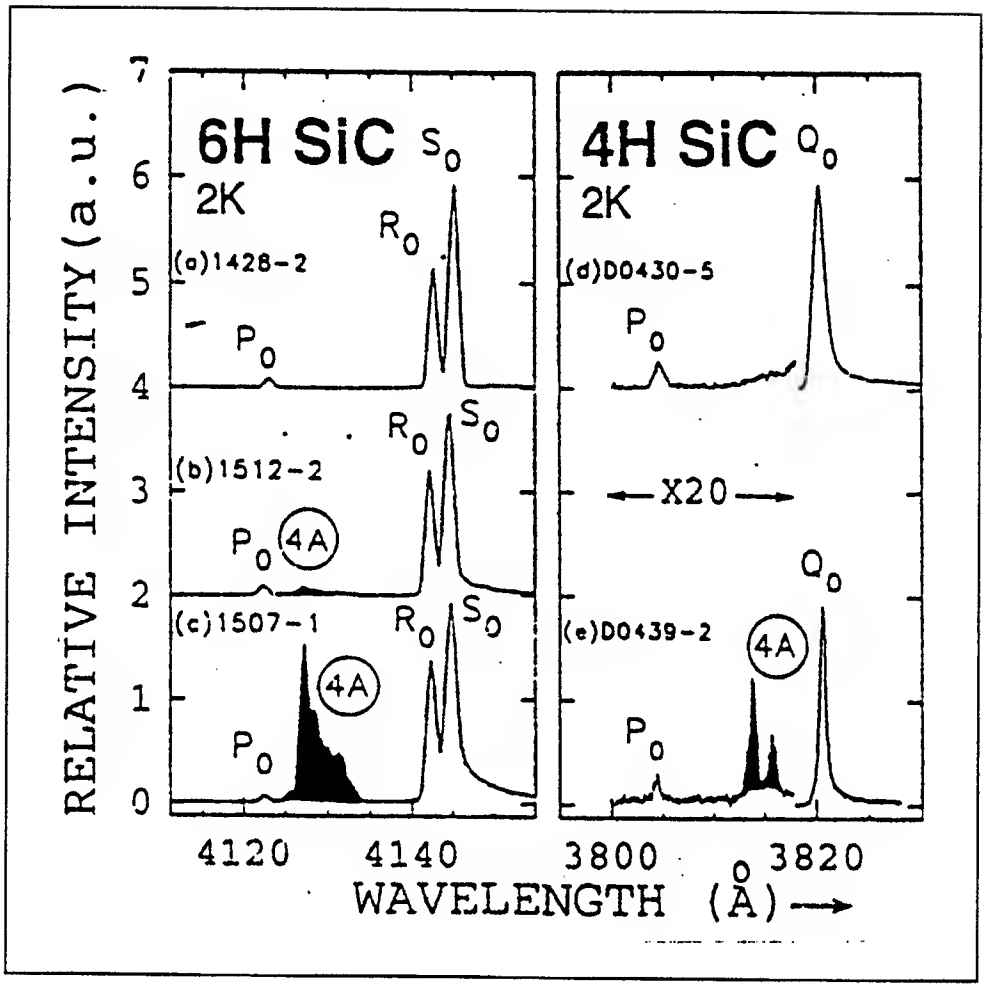

Figure 24: Low temperature photoluminescence spectra of 6H- and 4H-SiC thin films. The top two spectra are undoped while the others are intentionally doped with aluminum. The shaded areas are the no-phonon lines of the 4A complex. The estimated binding energy for 6H-SiC is between 18-23.4 meV.[17]

4.6 Infrared Spectra of Vanadium Deep Level Impurities in SiC

Another common residual transition impurity in SiC crystals grown by the sublimation process is vanadium. Vanadium occurs in multiple charge states, and deep energy levels are formed in the bandgap of SiC.[18] Figure 25 is a low temperature infrared photoluminescence spectrum of a Westinghouse 6H-SiC crystal grown by the sublimation process. All SiC crystals emit infrared in the 1.3-1.5μm range. Previous photoluminescence and electron spin resonance work shows the luminescence arises from intra-3d-shell transitions $^2T_2 \rightarrow {}^2E_2$, of $V_{si}^{4+}(3d^1)$.[18] Furthermore, it was shown in the same work that vanadium is amphoteric in SiC forming a deep acceptor state, $V_{si}^{4+}(3d^1) \rightarrow V_{si}^{3+}(3d^2)$, and a deep donor state, $V_{si}^{4+}(3d^1) \rightarrow V_{si}^{5+}(3d^0)$.[18]

The sharp line features in Figure 25 are typical for 6H-SiC with three ZPLs labeled α, β, and γ. The lines are assigned to sites with the α line at the hexagonal site and β and γ at the two quasi cubic sites. The α line is split into four components and this is believed to be caused by a stronger crystalline field acting on the hexagonal site. The source of the peak marked * is unknown and is still under investigation. Figure 26 is the low temperature infrared photoluminescence from a Westinghouse 4H-SiC sample. Only two sets of ZPLs are found and are labeled α for the hexagonal site and β for the cubic site. The splitting of the α line seen in 6H-SiC are also seen in 4H-SiC. For both polytypes, local phonon sidebands are also present. Table VI lists the positions of the vanadium lines for 4H- and 6H-SiC.

Table VI: List of luminescence lines associated with neutral vanadium in 4H and 6H-SiC. The units are in eV.

Polytype	α_1	α_2	α_3	α_4	*	β	γ	α_{2_90}	α_{3_90}
6H	.9463	.9455	.9441	.9433	.9231	.9150	.8913	.8603	.8563
4H	.9697	.9683	.9675		.9466	.9285			

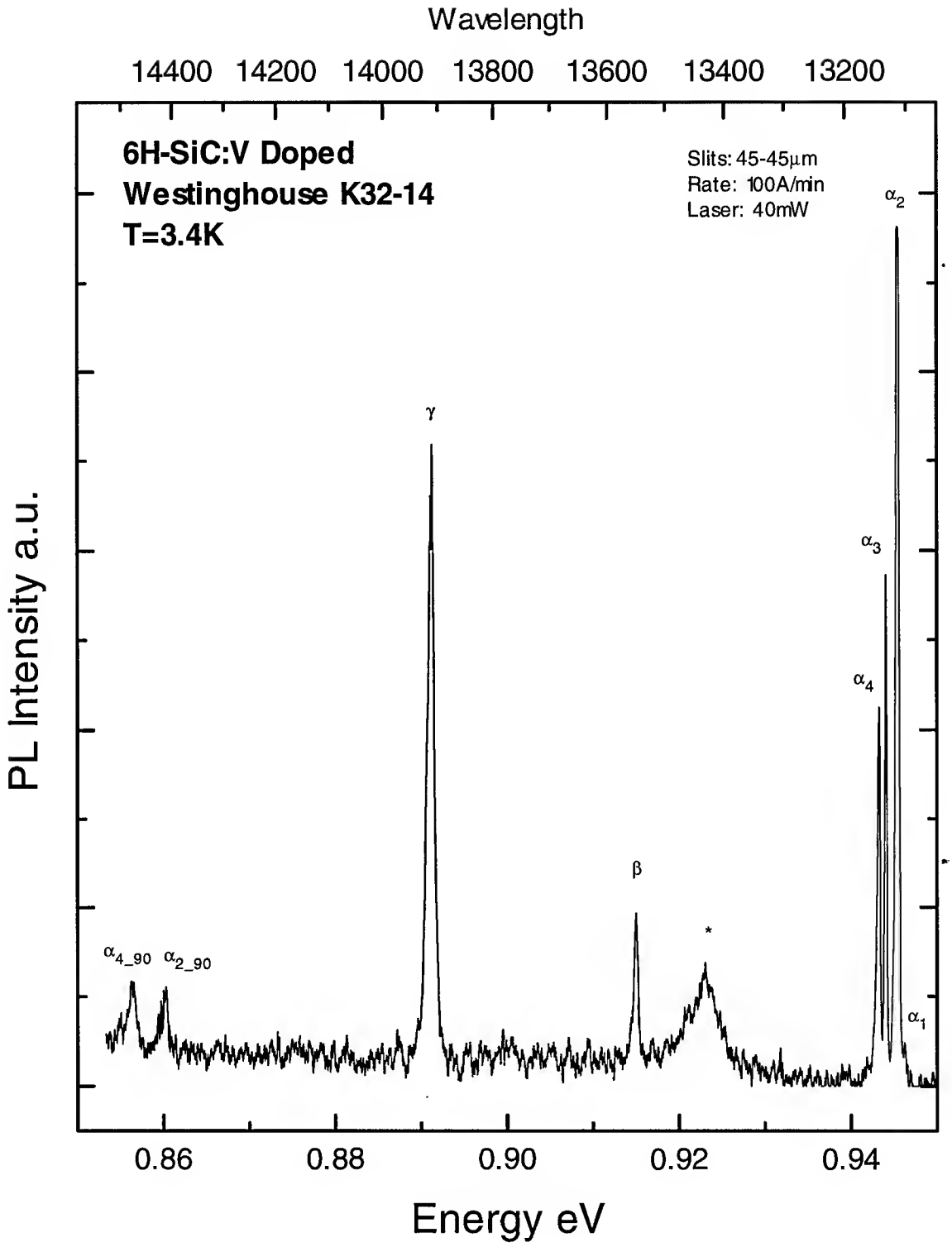

Figure 25: Low temperature photoluminescence spectrum of vanadium in 6H-SiC. The zero phonon lines arise from $^2T_2 \rightarrow {}^2E_2$ transitions of $V_{si}^{4+}(3d^1)$ occupying substitutional silicon sites.

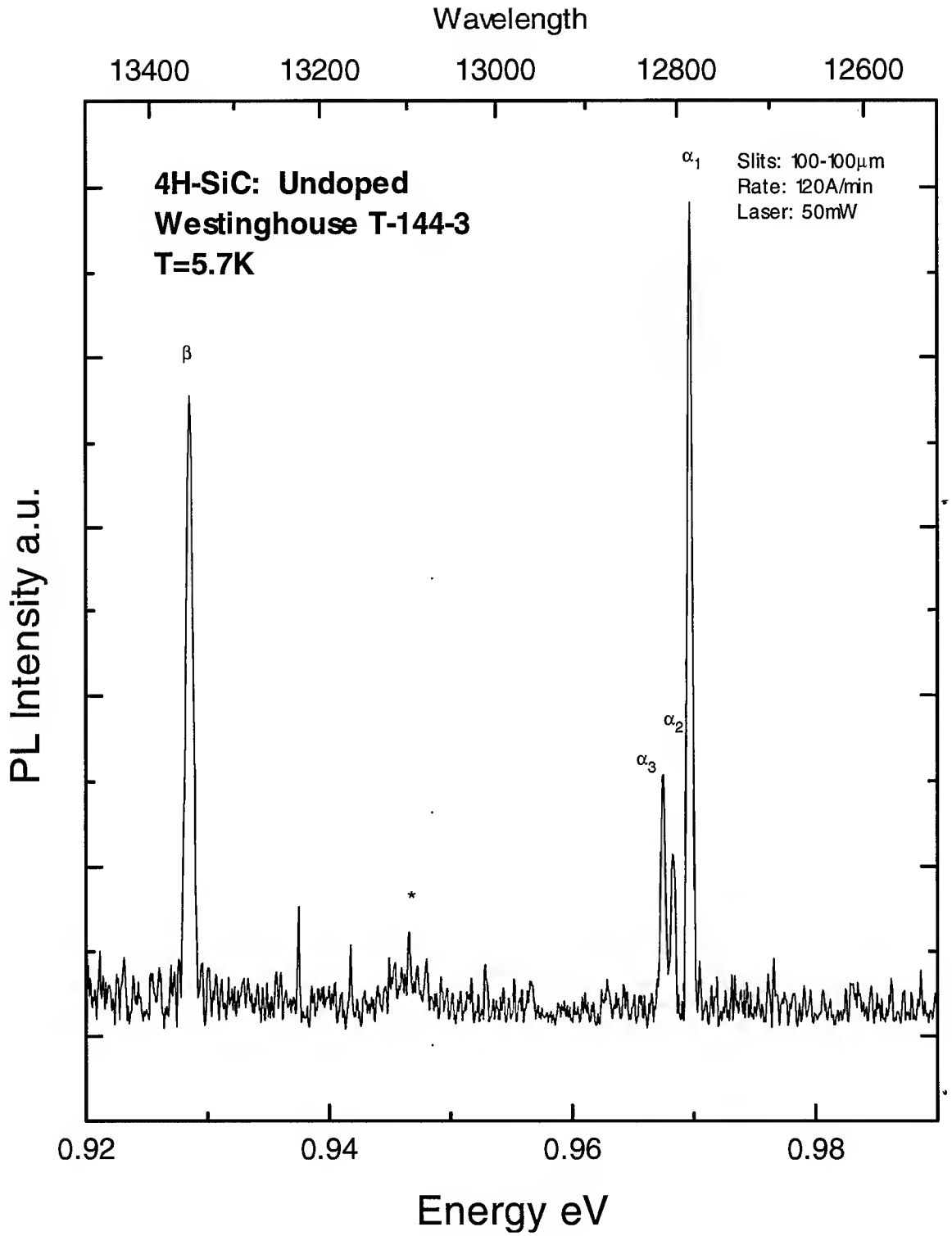

Figure 26: Low temperature photoluminescence spectrum of vanadium in 4H-SiC. The zero phonon lines arise from $^2T_2 \rightarrow {}^2E_2$ transitions of $V_{si}^{4+}(3d^1)$ occupying substitutional silicon sites.

5. Photoluminescence of Westinghouse 4H- and 6H-SiC

5.1 Overview

Low temperature photoluminescence data obtained on 4H- and 6H-SiC grown by the sublimation method at Westinghouse Science and Technology Center (WSTC) are presented here. The basic approach was to first observe each sample in the ultraviolet-visible region and then to observe each sample in the near-infrared spectral region. A total of ten SiC samples from WSTC were studied in both spectral regions.

5.2 6H-SiC Sample Results

Four undoped, two vanadium-doped, and one boron-doped 6H-SiC samples from WSTC were studied. For the undoped samples, the Ti bound exciton spectrum was the dominant luminescent center as seen in Figure 27. In all cases, the three ZPLs A_0, B_0, and C_0 are clearly distinguished in the spectra of the four undoped samples. Furthermore, all the spectra show a broad peak centered at approximately 2.50 eV which is due to the numerous phonon replicas of the bound exciton lines. This broad peak explains the intense green emission from these samples. Finally, the neutral nitrogen bound exciton spectrum was quenched at low temperature in the undoped samples possibly due to exciton hopping to the deeper Ti isoelectronic traps.

The visible region luminescence from the boron-doped 6H-SiC sample differed significantly from the undoped samples. Figure 28 shows the spectra from this sample which reveals a second broad peak in addition to the peak centered at 2.50 eV. This second peak is centered at approximately 1.90 eV with what appears to be a shoulder on the higher energy side at 2.0 eV. This peak is too low in energy to be related to N-B DAP luminescence previously observed by Ikeda and Matsunami. In addition, the peak is too low in energy to be N-D-center

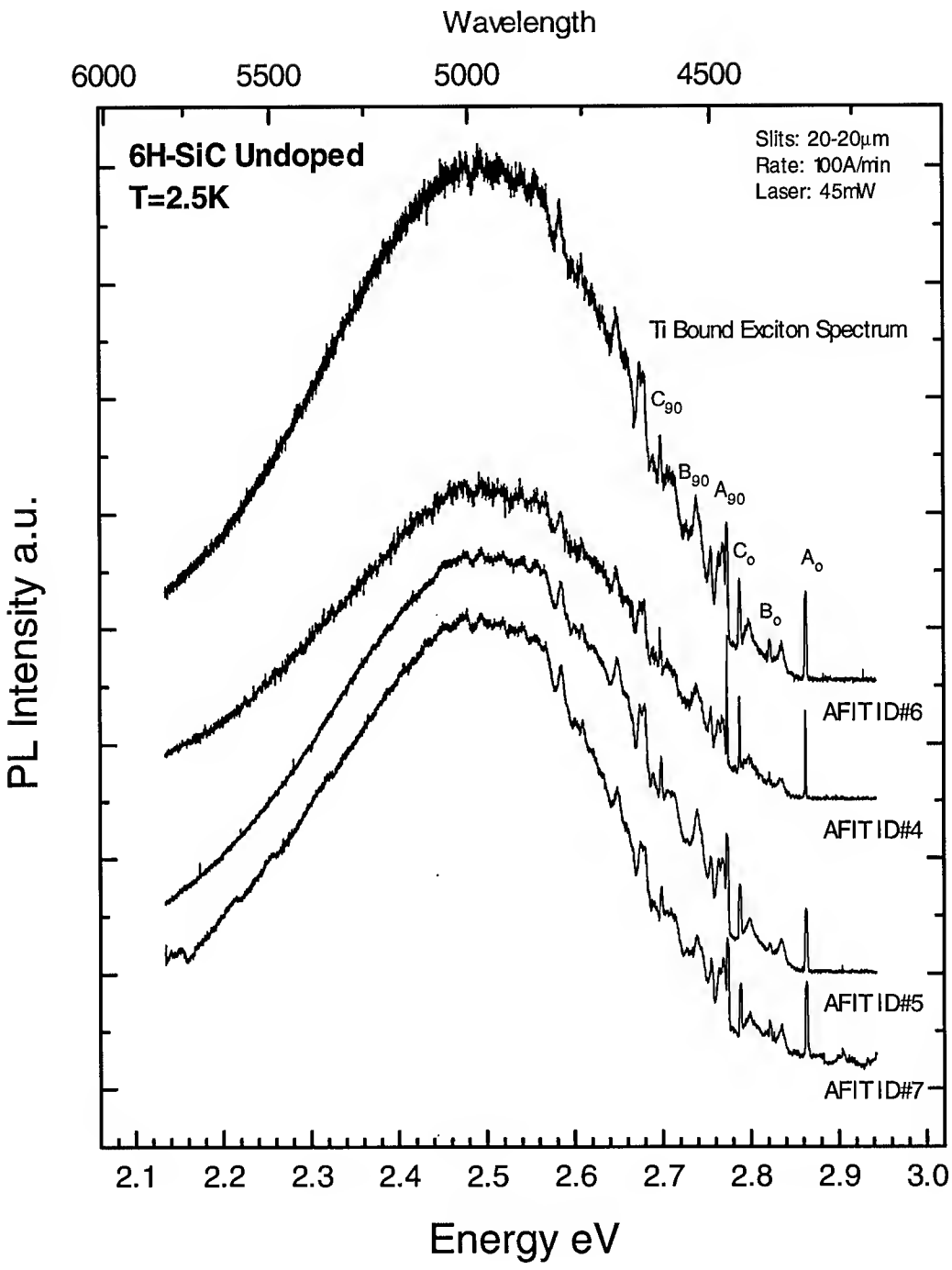

Figure 27: Low temperature photoluminescence from four undoped 6H-SiC samples from Westinghouse.

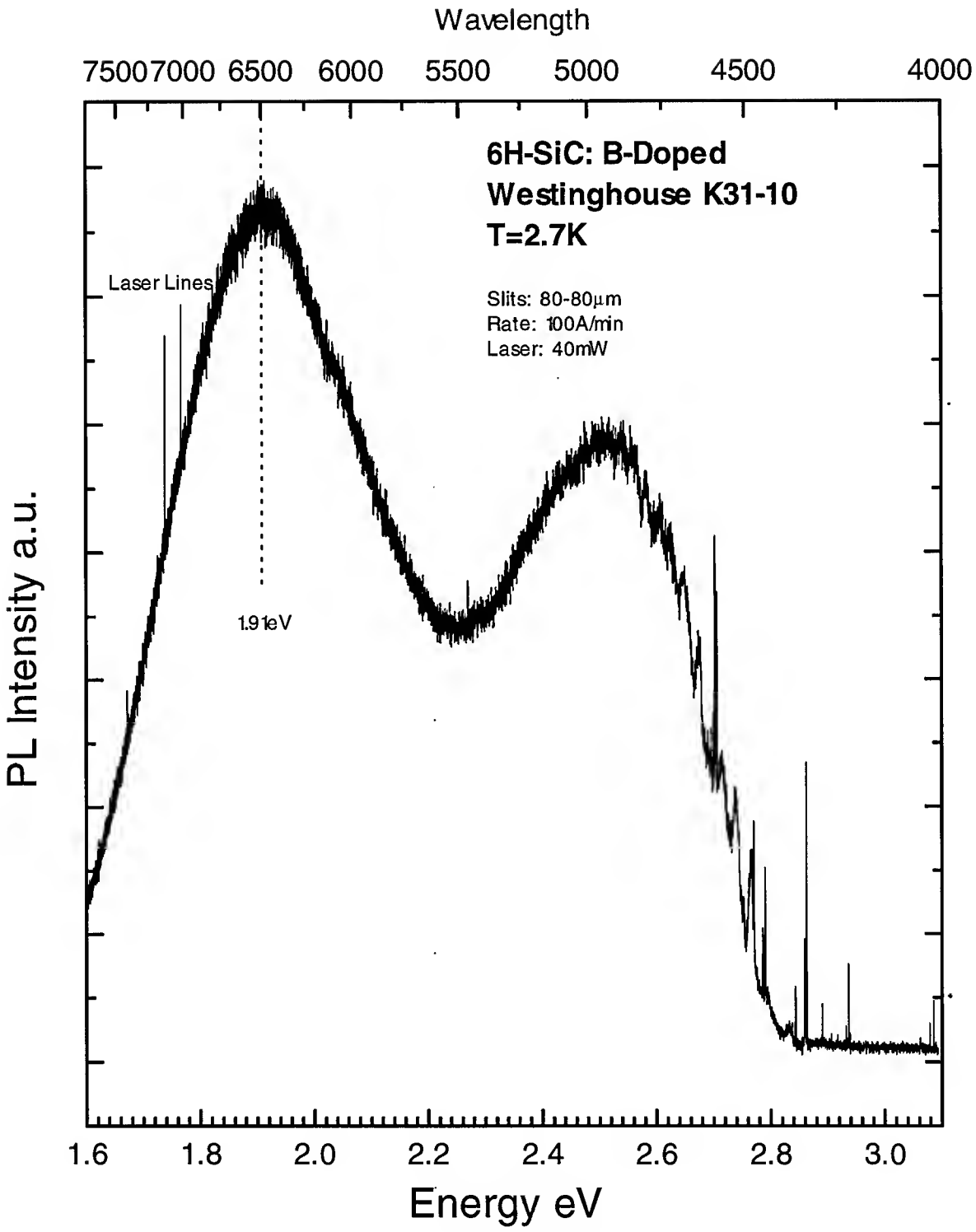

Figure 28: Low temperature photoluminescence from a 6H-SiC:B-doped sample from Westinghouse.

DAP luminescence observed at 2.0 eV by Suttrop and Pensl.[19] Thus, the origin of this peak is unknown, but it is believed to be related to the presence of boron.

The Ti bound exiton luminescence from the boron doped sample also differs from the undoped samples. Figure 29 shows the Ti spectrum in more detail and indicates the presence of additional lines on the lower energy side of A_0 and C_0 and their 90 meV local phonons. The sharpness of these lines and the presence of a related 90 meV local phonon strongly suggests they are bound exciton lines. The B_0 ZPL is missing from the luminescence which may explain the absence of a third related line and its 90 meV local phonon. The origin of these lines can possibly be attributed to the presence of an isotope of Ti in the crystal. Kemenade and Hagan used luminescence from various isotopes of Ti to prove the A_0, B_0, and C_0 lines were indeed due to Ti bound excitons.[11] They observed additional lines in the same energy region which they attributed to the presence of Ti isotopes. Thus, the presence of these additional lines in the same energy region as the Ti bound exciton luminescence may indicate the presence of an isotope of Ti in the sample.

The visible region luminescence from a vanadium-doped 6H-SiC sample is shown in Figure 30. The luminescence is almost the same as that seen for the boron-doped sample; however, the relative intensity of the 1.90 eV peak to the intensity of the 2.50 eV Ti related peak is not as large as it is in the boron-doped sample. The Ti bound exciton luminescence is also similar to that seen for the boron-doped sample because the additional lines on the lower energy side of A_0 and C_0 and their 90 meV local phonons are present in this vanadium-doped sample. The 6H-SiC:B-doped sample was grown in Westinghouse's chamber K; whereas, the 6H-SiC:V-doped sample was grown in chamber M. Therefore, no connection between an artifact of the

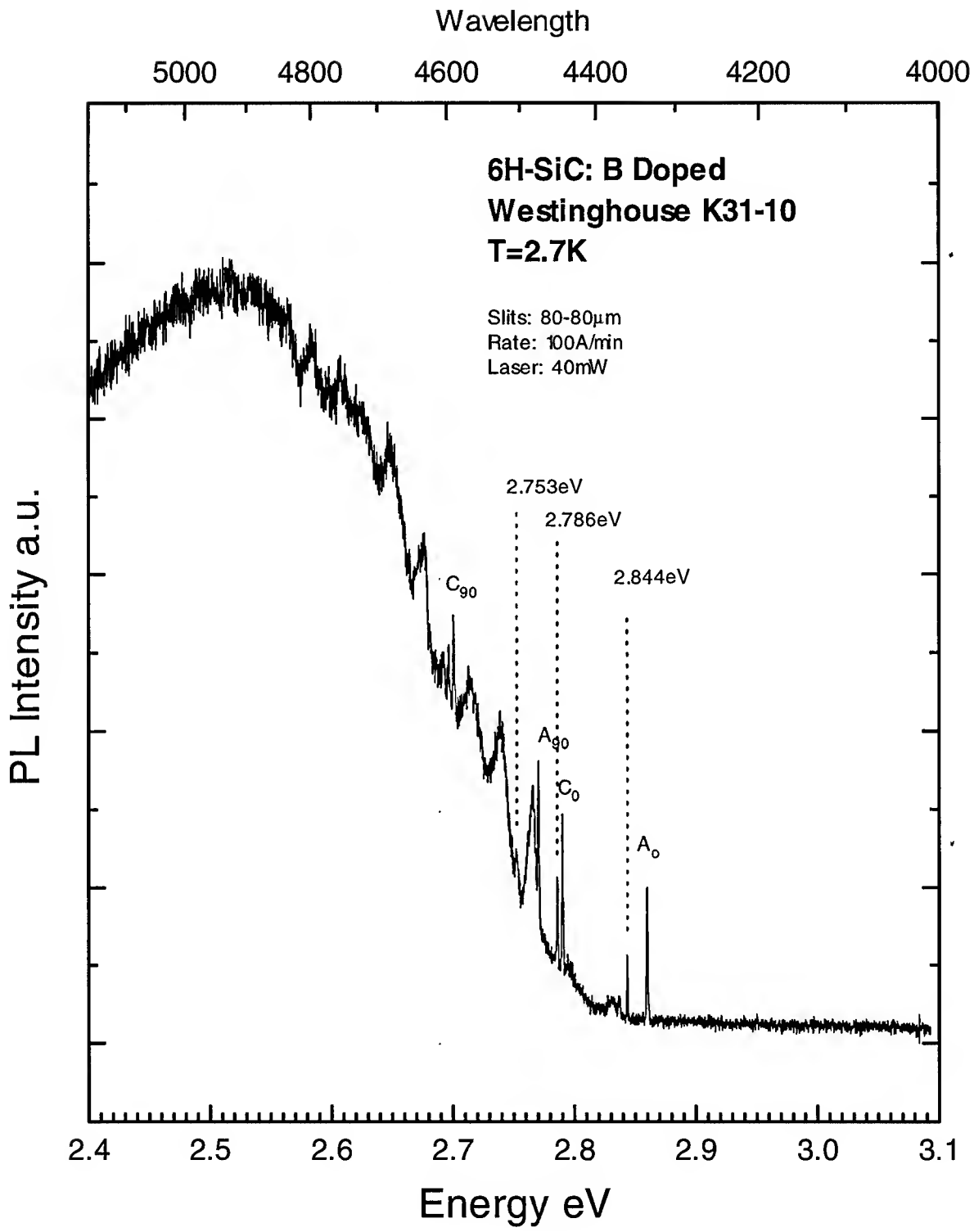

Figure 29: Close up view of the Ti-bound exciton luminescence from a 6H-SiC:B-doped sample. Notice the additional lines present in the Ti spectrum.

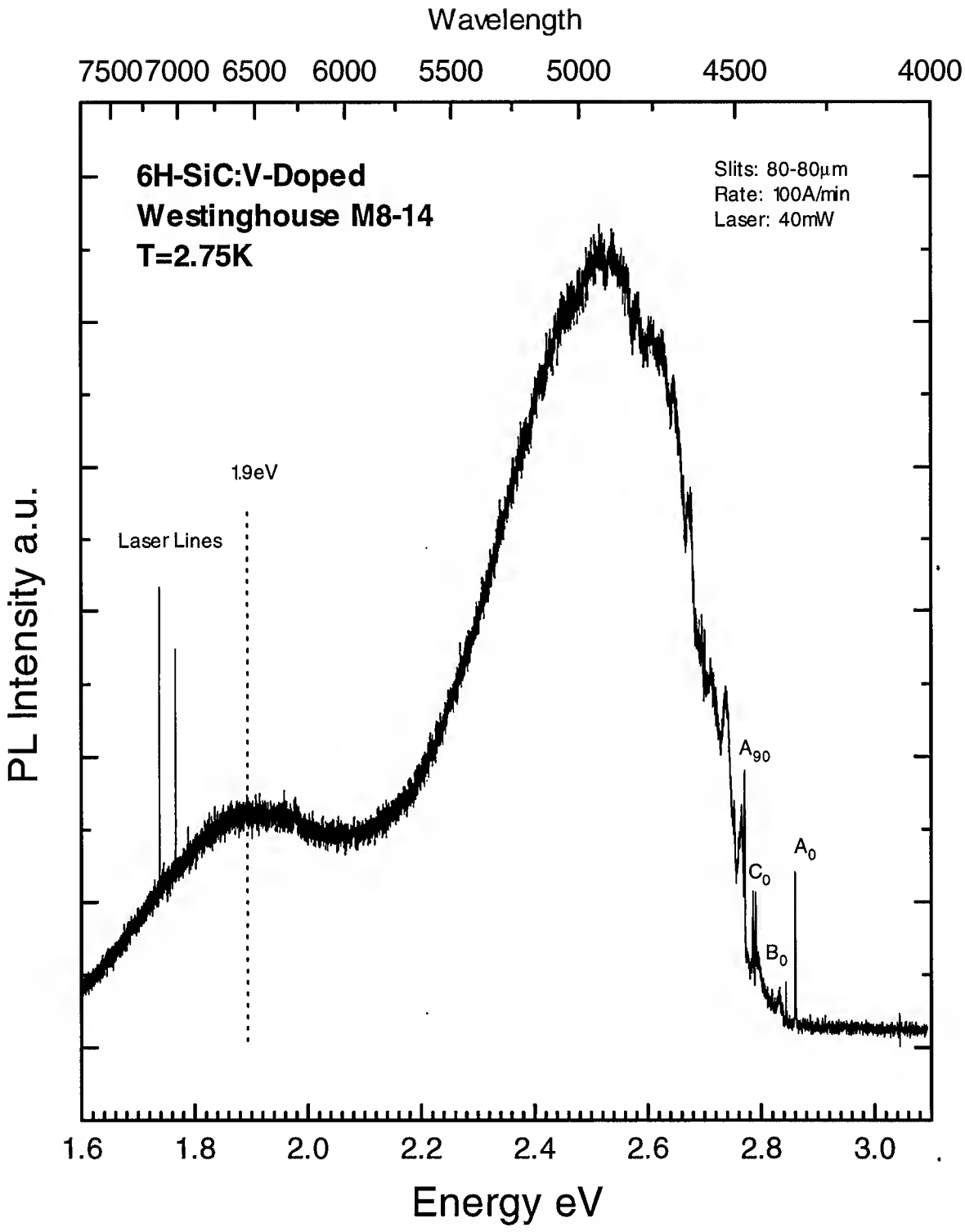

Figure 30: Low temperature photoluminescence from a 6H-SiC:V-doped sample from Westinghouse. Notice the broad peak centered at 1.90 eV similar to that seen in the 6H-SiC:B-doped sample.

growth chambers can be made to explain the presence of the additional lines seen for both these samples.

The luminescence from another 6H-SiC:V-doped sample is seen in Figure 31. The presence of aluminum in this sample is immediately noticeable due to the strong N-Al DAP luminescence. The quenching of the B series indicates the presence of large amounts of aluminum in the crystal as discussed in section 4.4. When the sample is strongly p-type due to aluminum acceptors, the fermi level lies near the acceptor level and the number of occupied donors in hexagonal sites is much less than those occupying cubic sites; thus, transitions due to N-donors in hexagonal sites are far fewer than transitions due to N-donors in cubic sites. This results in the quenching of the B series at low temperature in N-Al DAP recombination.

5.3 6H-SiC Near-Infrared Luminescence

The near-infrared low temperature photoluminescence from the 6H-SiC samples are presented in this section. The near-infrared luminescence from the four undoped 6H-SiC samples was difficult to detect due to the low intensity of the luminescence. Figure 32 shows the luminescence from an undoped sample The luminescence from the other undoped and B-doped samples are not shown but are similar in intensity and detail. Only two of the α-group lines related to the intra-3d-shell transitions of $V_{si}^{4+}(3d^1)$ at the hexagonal site are seen in the spectra. In addition, the unknown peak at $\approx$0.92 eV is barely above the background noise.

The luminescence from the vanadium-doped samples was much stronger, and Figure 33 shows the spectra for one of the vanadium doped samples. The luminescence from both vanadium-doped samples was equal in intensity and showed the same spectral features, so only one spectrum is represented.

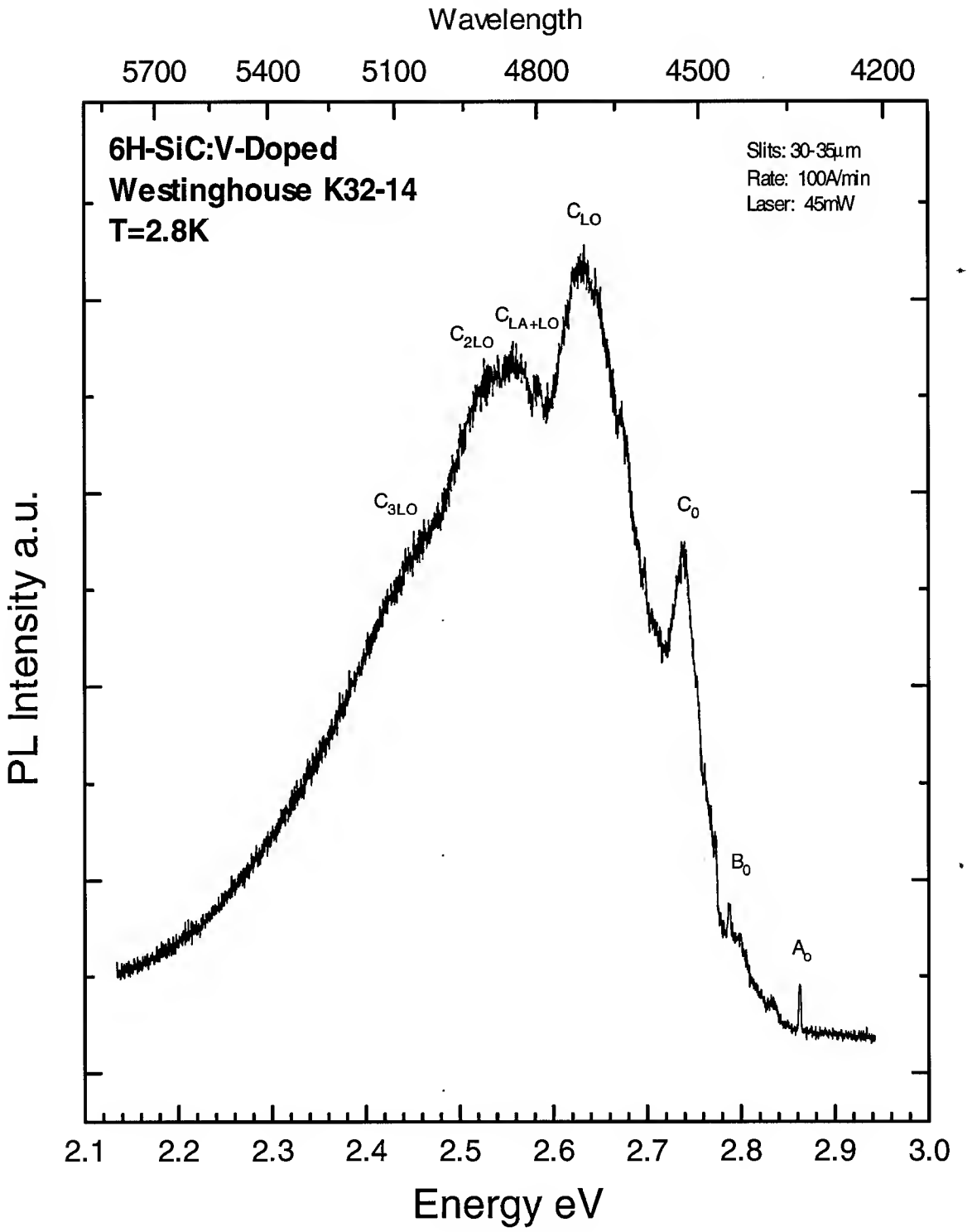

Figure 31: Low temperature photoluminescence of a 6H-SiC:V-doped sample. The luminescence indicates the presence of a significant amount of aluminum in the crystal due to the quenching of the B series. The subscripts indicate the kinds of phonons with $E_{LA} \approx 68$ meV and $E_{LO} \approx 107$ meV.

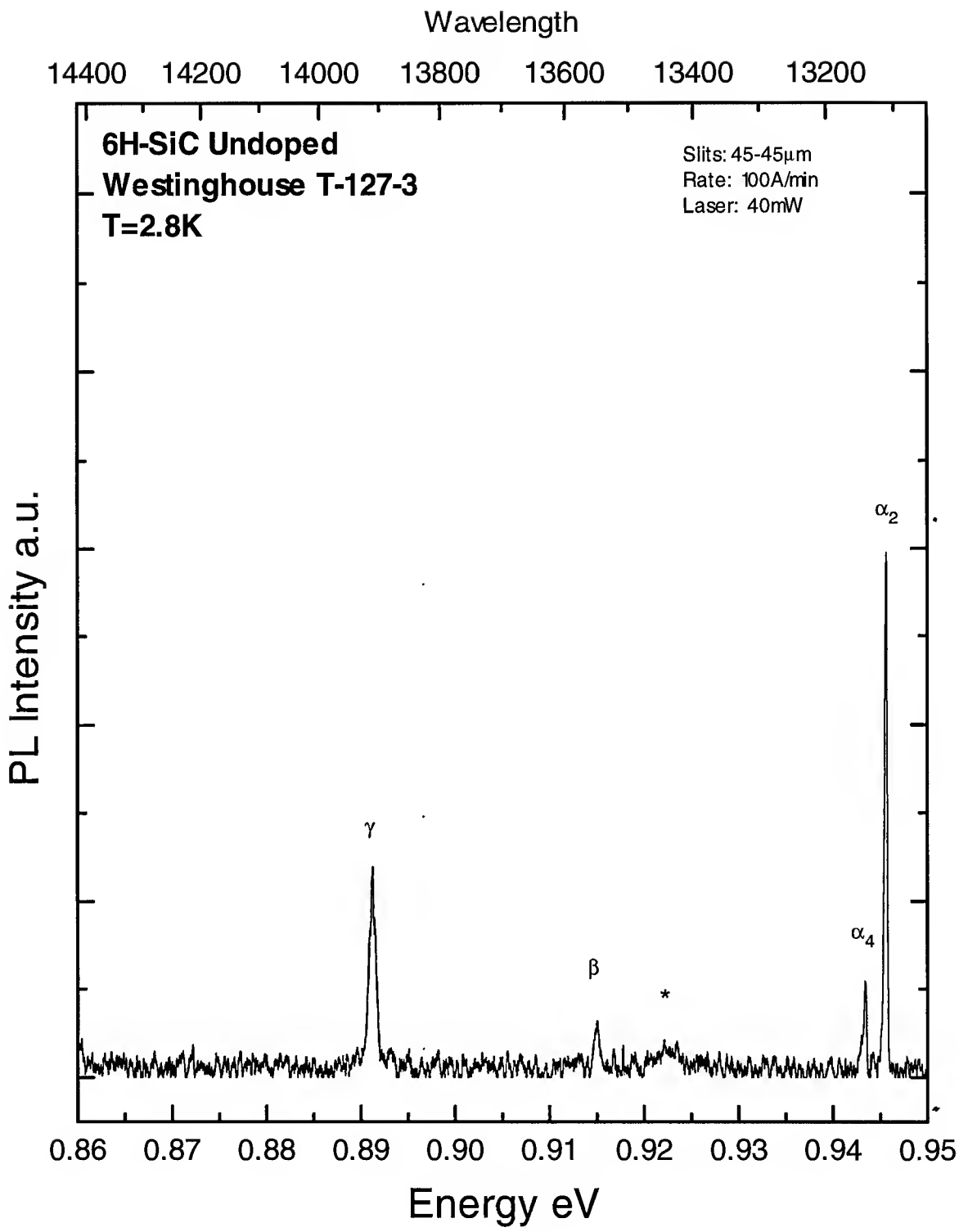

Figure 32: Near-IR luminescence from a 6H-SiC:Undoped sample. The luminescence was weak for all the undoped and the B-doped samples which had similar spectra to that seen here.

The spectral features of the vanadium-doped samples are markedly different than that seen for the undoped samples. All four lines associated with the α-group of vanadium related luminescence are clearly seen in Figure 33. Furthermore, the unknown peak at 0.92 eV and the β and γ peaks are more intense for the vanadium-doped samples. The luminescent intensity of the vanadium-doped samples is estimated to be at least ten times that of the undoped samples based on the data collection parameters. The output scale for the vanadium-doped samples was 10 mV and the scale for the undoped samples was 1 mV which indicates the signal is ten times larger for the vanadium-doped samples. The increase in luminescence intensity indicates the successful incorporation of vanadium into the crystal.

5.4 4H-SiC Visible Region Luminescence

This section describes the luminescence in the visible region from the three 4H-SiC samples from Westinghouse. One undoped, one N-doped, and one V-doped sample were studied. Figure 34 is the luminescence spectra from a 4H-SiC:N-doped sample from 2.1 to 3.2 eV. The luminescence is dominated by the Ti-bound exciton recombination. The bound exciton lines A_0 and B_0 and their related 90 meV local phonons are clearly distinguishable in the luminescence. Moreover, no nitrogen spectrum was observed possibly due to large Ti contamination of the crystal during growth. The broad peak centered at 2.45 eV is due to the multiple phonon replicas of the Ti-bound excitons.

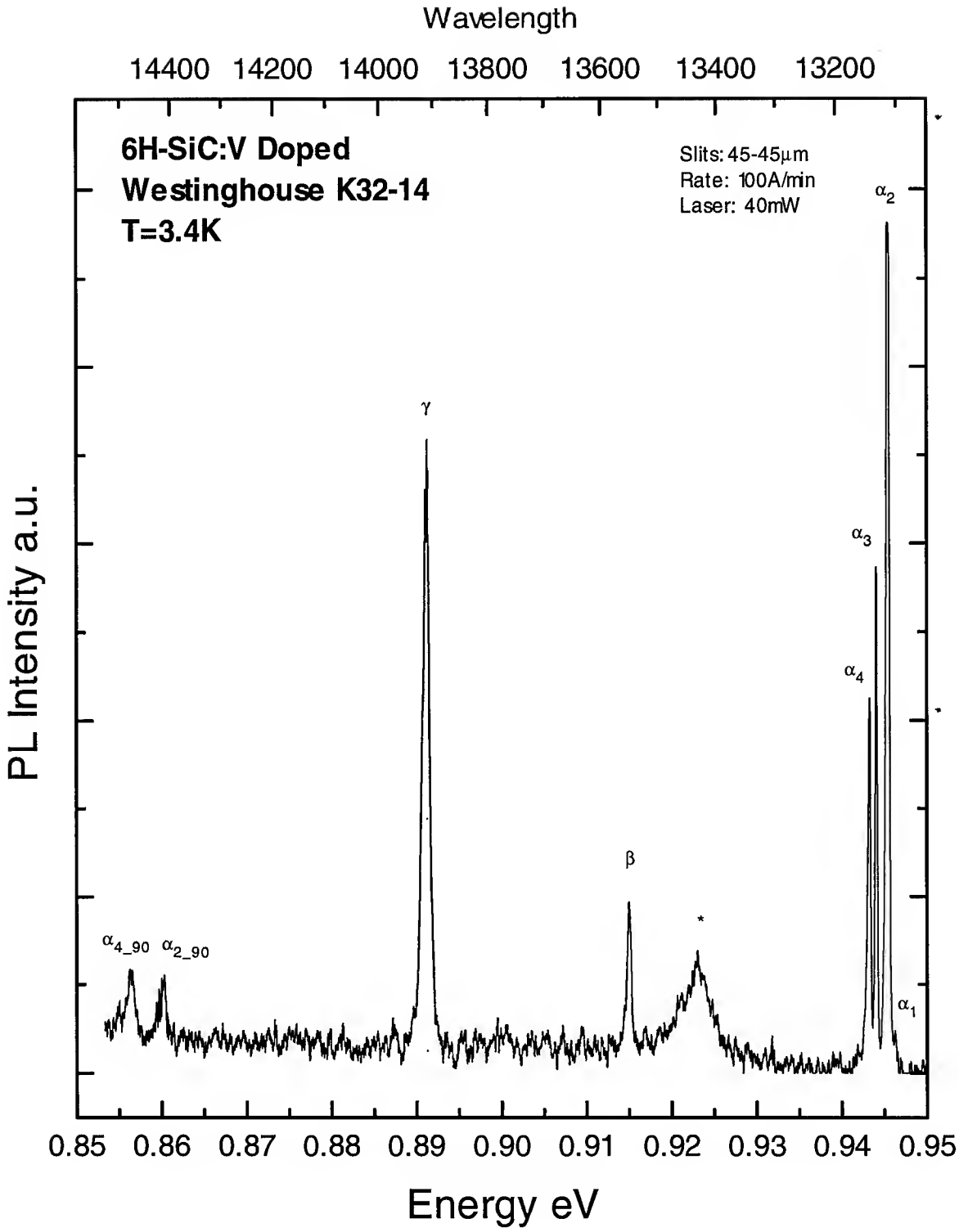

Figure 33: Near-IR luminescence from a 6H-SiC:V-doped sample. The intensity of the luminescence was an order of magnitude greater for the vanadium-doped samples compared to the undoped samples in Figure 33.

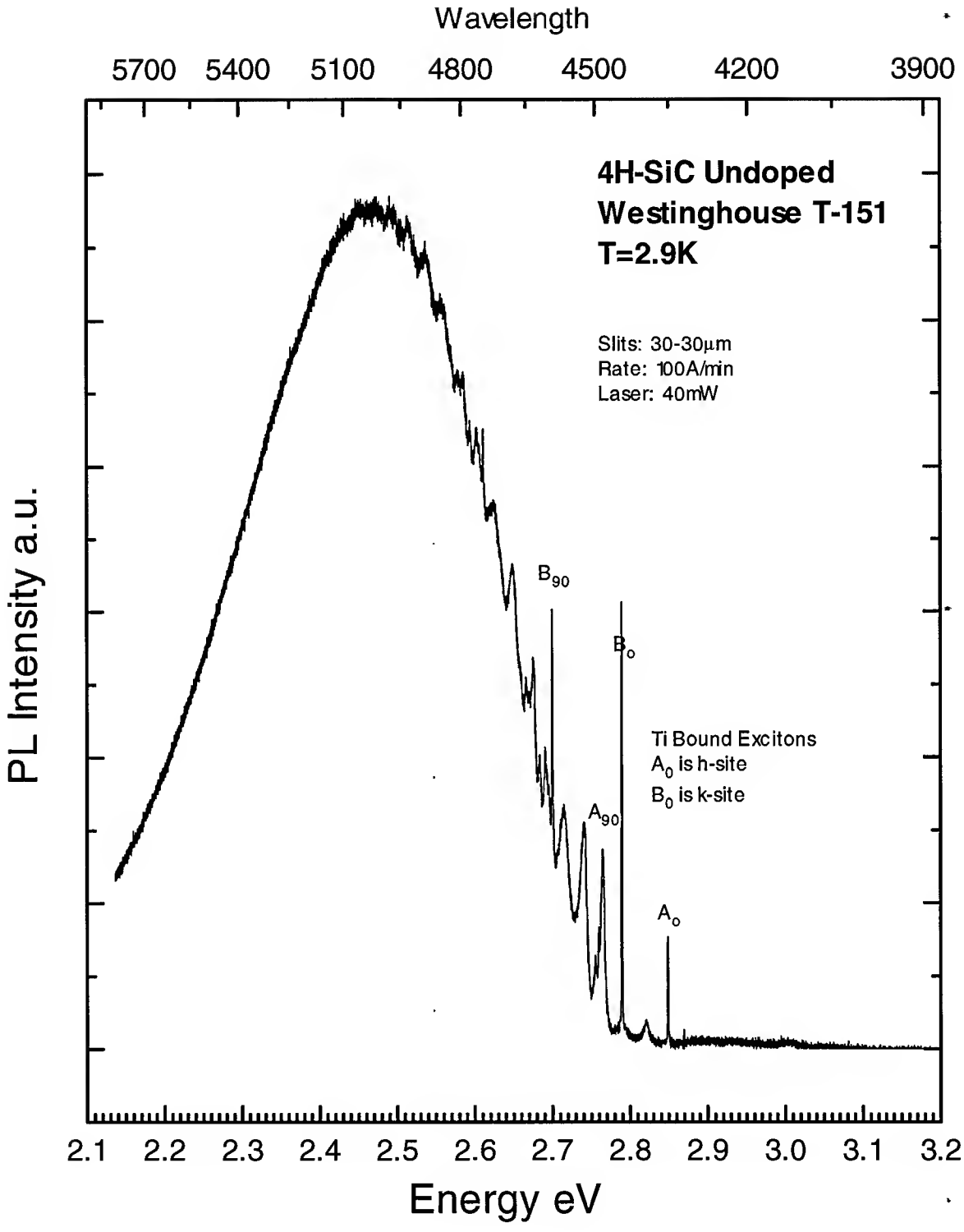

Figure 34: Low temperature photoluminescence from 4H-SiC:N-doped from Westinghouse. The spectrum is dominated by the Ti-bound exciton and related phonon luminescence.

The luminescence from a 4H-SiC undoped sample is shown in Figure 35. The spectrum is quite different from that seen in Figure 34 due to the N-Al DAP spectrum and the absence of the Ti - bound exciton spectrum and its associated broad phonon peak at 2.50 eV. The N-Al DAP spectrum seen in Figure 35 is typical for 4H-SiC with even small amounts of aluminum in the crystal due to the higher probability for N-Al DAP transitions. The presence of the broad peak centered at 2.19 eV, however, is very similar to the presence of the broad peak at 1.90 eV for 6H-SiC:B-doped. The bandgap of 4H-SiC is approximately 240 meV greater than 6H-SiC's bandgap. The 240 meV difference is about the same magnitude for the difference in location of the two broad peaks seen in each polytype. Thus, the centers responsible for this broad peak in both polytypes are likely the same center.

The luminescence from the only 4H-SiC:V-doped sample studied is seen in Figure 36. In this sample, what appears to be a contribution from N-Al DAP transitions is seen between 2.8 to 3.1 eV. The relative peak heights expected for DAP luminescence in 4H-SiC are not seen in this spectra, but the energy location of the peaks corresponds well for N-Al DAP luminescence. The rest of the spectrum is dominated by the Ti-bound exciton recombination and the associated broad multi-phonon replica peak at 2.45 eV. Absent from this sample is the broad peak at 2.19 eV seen for the undoped sample.

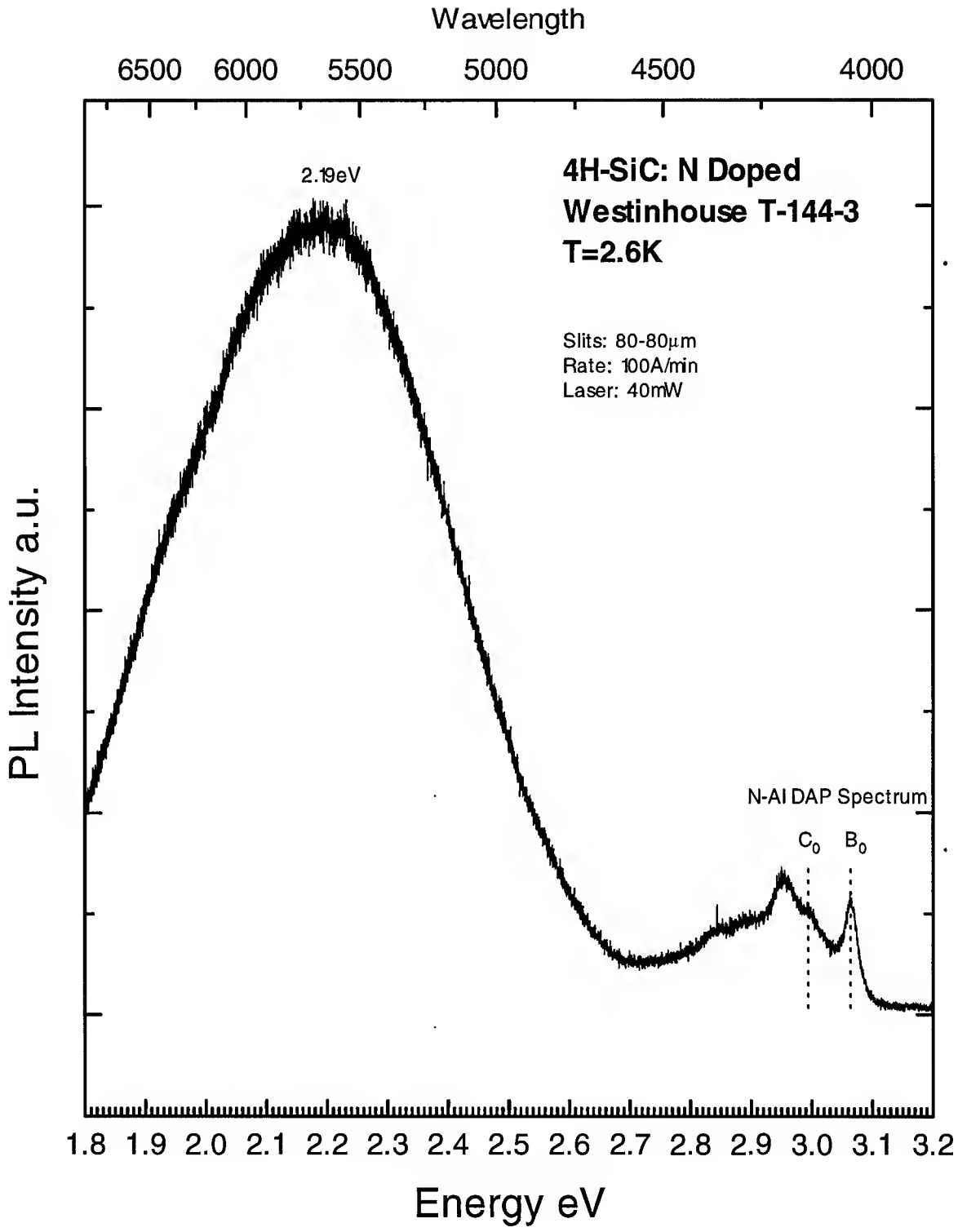

Figure 35: Low temperature luminescence from a 4H-SiC:undoped sample from Westinghouse. The N-Al DAP luminescence is present as well as the broad peak at 2.19 eV similar to the peak at 1.90 eV for 6H-SiC:B-doped.

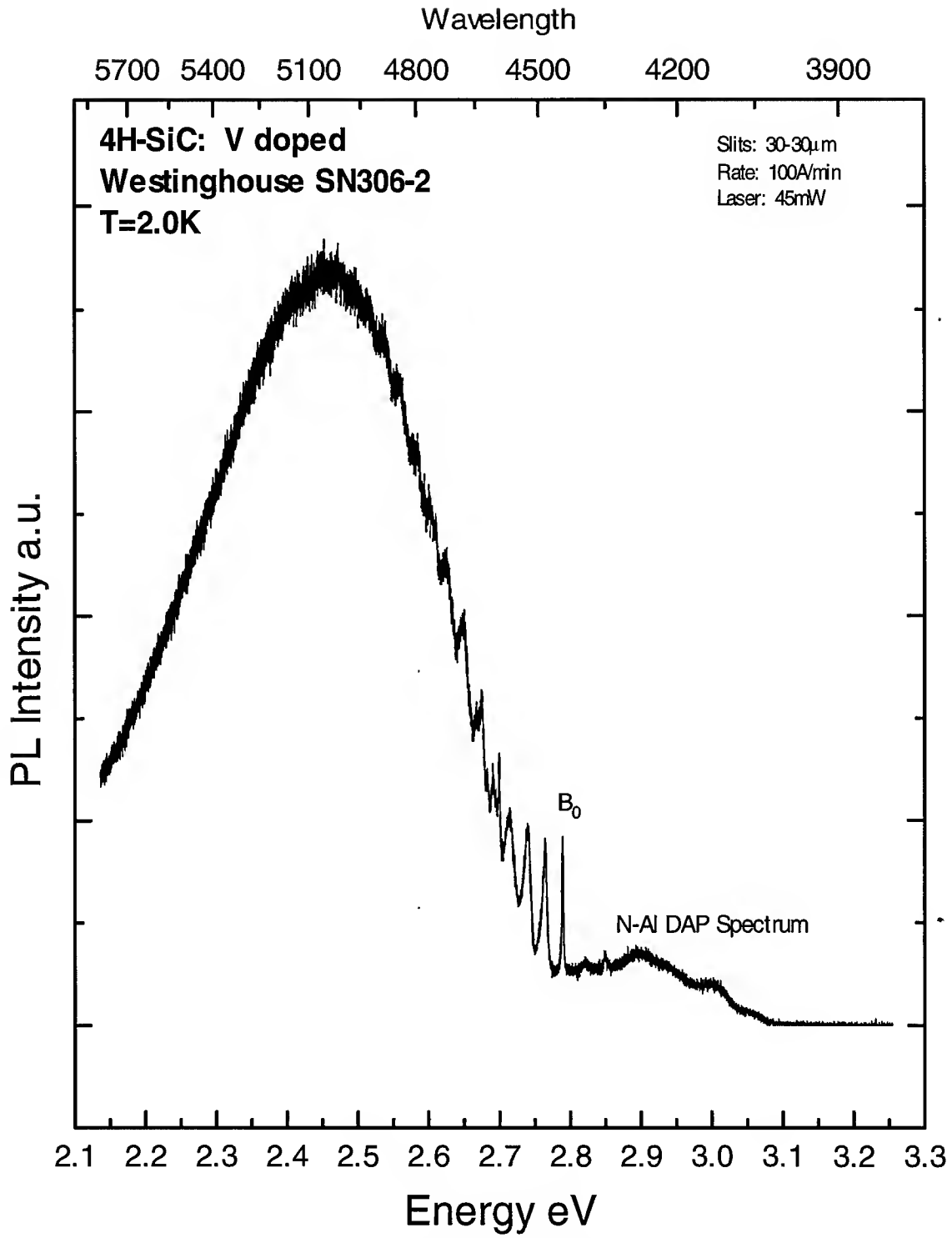

Figure 36: Low temperature luminescence from a 4H-SiC:V-doped Westinghouse sample. Suppressed N-Al DAP peaks are present along with the Ti-bound exciton luminescence. No broad peak at 2.19 eV was observed.

5.5 4H-SiC Near-IR Region Luminescence

The near-IR luminescence from an undoped 4H-SiC sample is seen in Figure 37. Both the undoped and N-doped samples had similar spectra in the near-IR in relation to luminescence intensity and structure. The signal was very weak for these samples as compared to the vanadium-doped sample. The signal intensity ratio was similar to the 6H-SiC samples with the vanadium doped sample on the 10 mV scale and the undoped samples on the 1 mV scale. Similar spectral features were seen in both undoped and doped samples, but the increase in luminescence intensity for the vanadium-doped sample is believed to be due to the increased amount of vanadium in the crystal much like the case for vanadium in 6H-SiC.

5.6 Related Optical Admittance Spectroscopy Measurements

All of the samples were studied by Optical Admittance Spectroscopy (OAS) by Dr. William Mitchel at Wright Laboratory, Materials Directorate. OAS of Schottky diodes made of 6H-SiC has the sensitivity of other capacitance techniques such as Deep Level Transient Spectroscopy; however, the high temperatures necessary to charecterize deep traps in wide bandgap semiconductors with DLTS is negated by OAS. In OAS, the junction is modulated with a sinusoidal voltage of frequency ω, and excitation from deep levels can occur when the Fermi level intersects the deep level. If the carriers are thermally emitted from the deep level, the carriers will create an additional conductance and capacitance; however, thermally emitted carriers are negligible at the temperature of the diode, typically 300°C. In OAS, the additional conductance and capacitance are created by the optical emission of carriers from the deep level. Peaks in the conductance occur when the energy of incident photons correspond to the transition energy of the deep level to the conduction band.

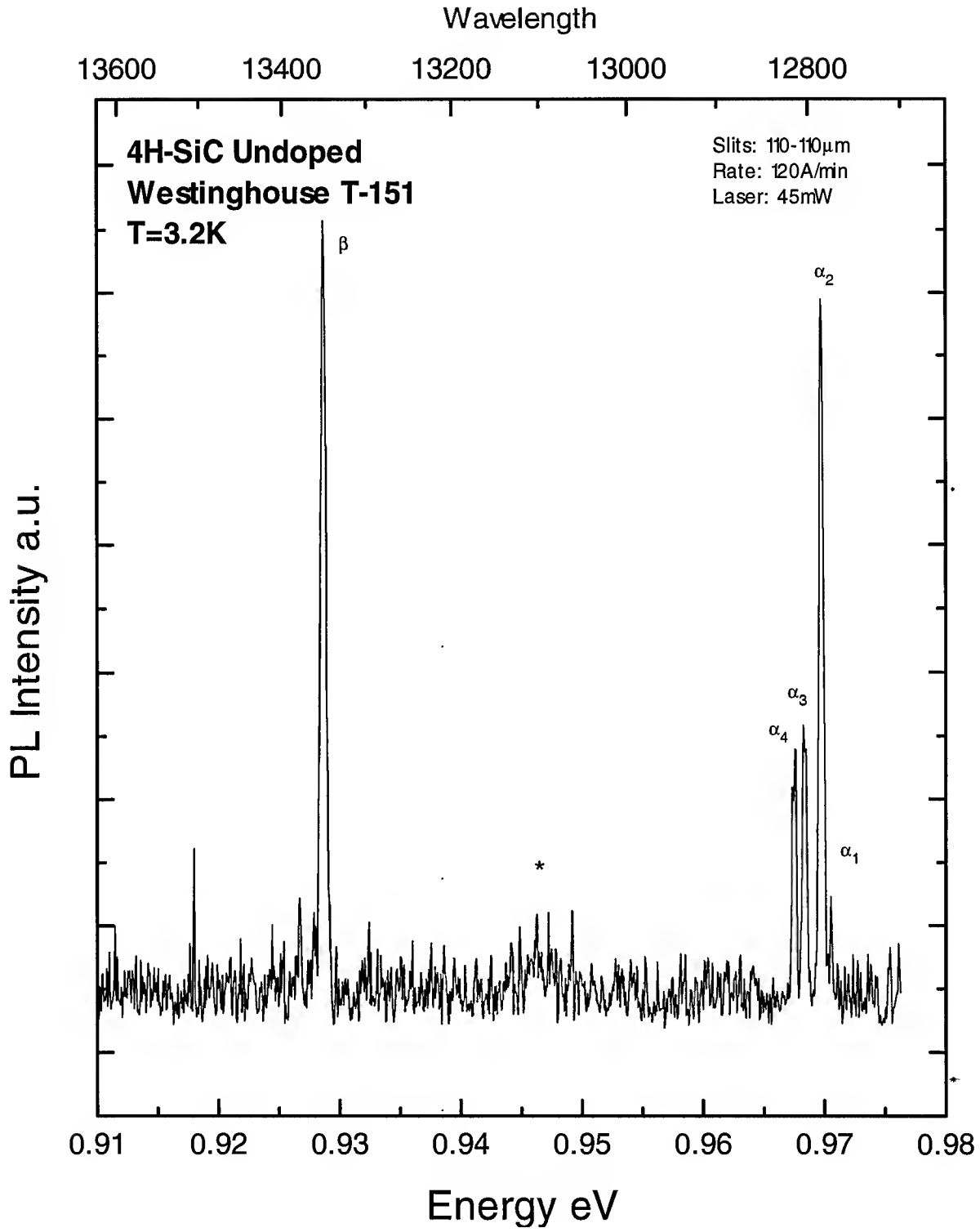

Figure 37: Near-IR luminescence from a 4H-SiC:Undoped sample. The luminescence intensity was very weak for the unintentionally vanadium-doped samples.

Figure 38 is a typical Optical Admittance spectrum for a 6H-SiC sample, and five peaks are clearly distinguishable. The band-to-band transition is marked at 3.10 eV, along with two peaks at 1.59 eV and 0.78 eV which Mitchel tentatively attributed to the donor and acceptor states of V_{Si}.[3] The identification of the 1.07 eV and 0.94 eV peaks were most likely due to other transition metal impurities in the material. The identification of the 0.78 eV peak was in question because the transition energy was close to the reported location of the Ti_{Si}-N_C complex of E_C-0.6 eV which was reported in photo-Electron Spin Resonance measurements.[20]

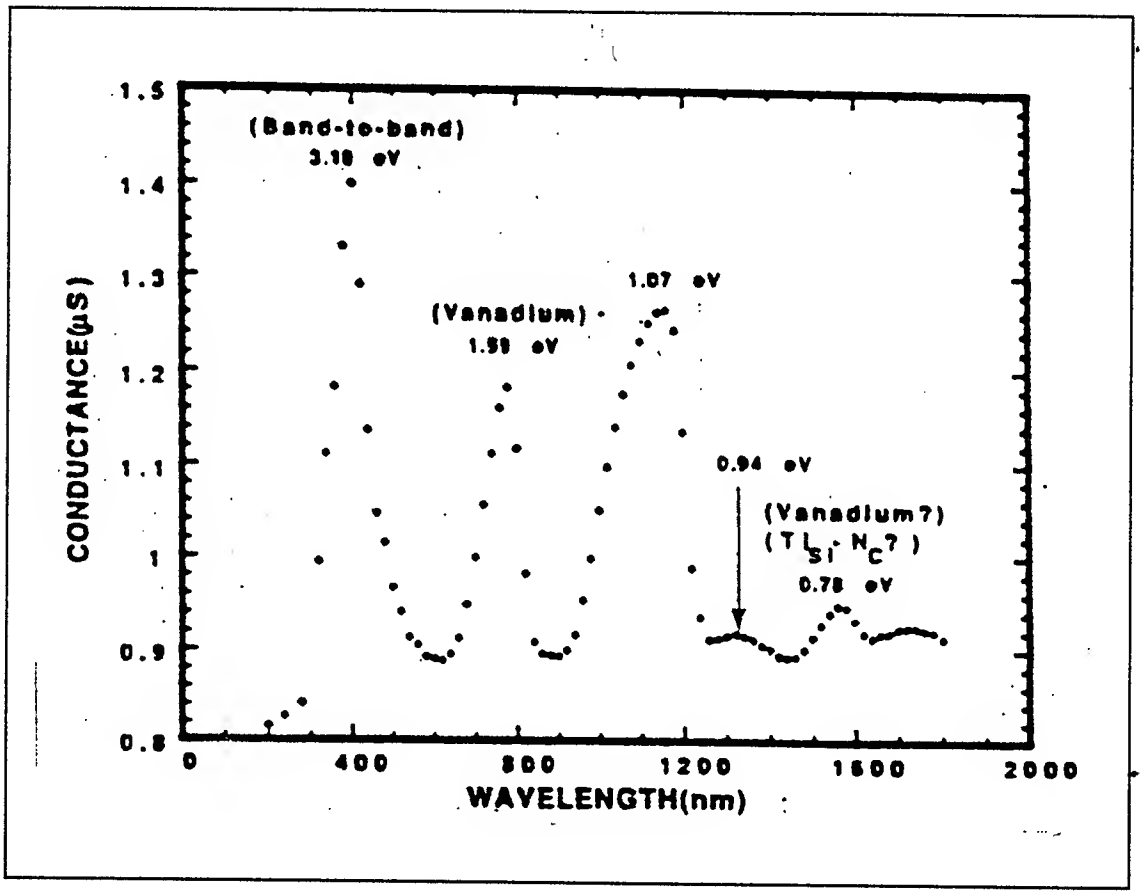

Figure 38: Optical Admittance Spectrum for 6H-SiC.

6. Conclusions

6.1 Conclusions

A set of low temperature photoluminescence data from various 4H- and 6H-SiC samples grown at Westinghouse Science and Technology Center has been presented. From this set of data, identification of impurity centers in the crystals was possible. In the visible spectral region, it was found the Ti-bound exciton recombination dominated the luminescence from most Westinghouse SiC samples. However, in samples #8 and #14 the N-Al DAP recombination was the dominant luminescence process. In fact, sample #8 is believed to be heavily doped based on the disappearance of the B series which indicates heavy Al-doping.

The appearance of a broad peak at ≈1.90 eV for 6H-SiC and ≈2.19 eV for 4H-SiC indicates the individual centers responsible for these peaks is indeed the same center when the change in bandgap, ≈240 meV, of the polytypes are considered. Furthermore, this dependence on the conduction-band location indicates a possible link with the nitrogen donor level which is strongly tied to the conduction band. The strong intensity of the 1.90 eV peak in a 6H-SiC:B-doped sample further indicates a possible link with boron; however, N-B DAP recombination has been ruled out because this was observed in previous reports at about 2.2 eV in 6H-SiC[16]. The large Ti contribution to the luminescence spectrum in these samples might lend a clue to the nature of the 1.90 eV peak. Titanium substituting for Si has been observed by photo-ESR to complex with nitrogen which substitutes for carbon in the lattice. The photo-ESR measurements found a Ti_{Si}-N_C nearest neighbor pair to act as a deep donor.[21] This deeper donor acting with the boron related defect center level at E_V+0.660 eV may be responsible for the 1.90 eV peak. If this was the case, the Ti_{Si}-N_C donor level would be determined by equation (3).

$$E_D = E_G - E_B - h\nu \qquad (3)$$

Where E_D is the ionization energy of the Ti_{Si}-N_C donor, E_G is the bandgap for 6H-SiC ≈3.1 eV, E_B is the ionization energy of the boron related defect center, and hν is the 1.90 eV peak energy. Based on these assumptions, for the 1.90 eV peak to be a Ti_{Si}-N_C-boron related defect DAP transition, the Ti_{Si}-N_C complex would be located at E_C-0.54 eV.

As discussed in Section 5.6, OAS experiments performed on these samples at Wright Laboratory did not find any deep level associated with a boron related acceptor at E_V+0.66 eV. However, deep levels at 0.78 eV, 0.94 eV, 1.07 eV, and 1.54 eV were reported in these samples. The 0.78 eV deep level closely corresponds with the location of the previously reported Ti_{Si}-N_C complex at E_C-0.60 eV[21]; however, none of the other deep levels can account for the luminescence seen at 1.90 eV in the Westinghouse samples. Thus, DAP recombination between a Ti_{Si}-N_C donor and a boron related D-center acting as an acceptor may be responsible for the 1.90 eV peak in 6H-SiC. By locating the boron related D-center at E_V+0.66 eV, the Ti_{Si}-N_C complex would have to be located at E_C-0.54 eV for the 1.90 eV peak to be a Ti_{Si}-N_C-boron related D-center DAP transition.

An excitation energy dependence on this peak would verify if this peak was indeed due to DAP recombination. When the excitation energy is increased, the peak energy should shift to higher energies as the recombination at distant pairs becomes more probable. Unfortunately, an increase of one-hundred times in incident power is typically necessary to see any significant shift in the peak energy, and an ultraviolet laser with this capability was not available in this study.

Finally, it was determined from the near-infrared luminescence spectra of 4H- and 6H-SiC that Westinghouse is successfully incorporating vanadium into the crystal. This conclusion was based on the increase, by an order of magnitude, of the luminescence intensity of the intra-3d-shell transitions for samples intentionally doped with vanadium compared to the unintentionally doped samples. The successful doping of vanadium into SiC by Westinghouse has reportedly resulted in 6H-SiC material with a resistivity of 10^7 Ω-cm which is semi-insulating.[6] However, it still remains to be shown that the compensation of the residual impurities is due to the presence of a vanadium deep level in the bandgap of 6H-SiC.

Bibliography

1 . H. Morkoc, S. Strite, G. B. Gao, M. E. Lin, B. Sverdlov, and M. Burns, J. Appl. Phys. **76**, 1363 (1994).

2 . R. J. Trew, J. B. Yan, and P. M. Hook, Proc. IEEE **76**, 598 (1991).

3 . W. C. Mitchel, Matthew Roth, S. R. Smith, A. O. Evwaraye, and J. Solomon, "Deep Levels in Undoped Bulk 6H-SiC and Associated Impurities: Application of Optical Admitance Spectroscopy to SiC.", Paper Presented at the Int'l Symposium on Compound Semiconductors, San Diego CA, Sep 1994.

4 . J. A. Powell and L. G. Matus, "Recent Developments in SiC", *Amorphous and Crystalline Silicon Carbide*, Springer Proceedings in Physics, Springer-Verlag Berlin, Vol. 34, 1989.

5 . Lyle Patrick, Phys. Rev. **127**, 1878 (1962).

6 . Westinghouse STC. *Technology for High Temperature Electronics: SiC for X-Band.* Annual Report. Pittsburgh: Westinghouse STC, April 1994.

7 . W. J. Choyke and Lyle Patrick, Phys. Rev. **127**, 1868 (1962).

8 . D. R. Hamilton, W. J. Choyke, and Lyle Patrick, Phys. Rev. **131**, 127 (1963).

9 . *Semiconductors: Group IV Elements and II-V Compunds.* Berlin: Springer-Verlag Berlin Heidelberg, 1991.

10 . P. J. Dean and R. L. Hartman, Phys. Rev. **B5**, 4911 (1972).

11 . A. W. C. van Kemenade and S. H. Hagen, Solid State Communications **14**, 1331 (1974).

12 . L. Patrick and W. J. Choyke, Phys. Rev. **B5**, 5091 (1974).

13 . Priscilla J. Colwell and Miles V. Klein, Phys. Rev. B **6**, 498 (1972).

14 . S. H. Hagen and A. W. C. van Kemenade, Journal of Luminescence **8**, 18 (1973).

15 . M. Ikeda, H. Matsunami and T. Tanaka, Journal of Luminescence **20**, 111 (1979).

16 . M. Ikeda, H. Matsunami and T. Tanaka, Phys. Rev. B **22**, 2842 (1980).

17 . L. L. Clemen, R. P. Devaty, M. F. MacMillan, M. Yoganathan, and W. J. Choyke, Appl. Phys. Lett. **62**, 2953 (1993).

18 . J. Schneider, H. D. Muller, K. Maier, W. Wilkening, andF. Fuchs, Appl. Phys. Lett. **56**, 1184 (1990).

19 . W. Suttrop, G. Pensl, and P. Lanig, Appl. Phys. A **51**, 231 (1990).

20 . K. Maier, Schneider J., Wilkening W., Leibenzeder S., Stein R., Mat'l Sci. Eng. **B11**, 27 (1992).

21 . J. Schneider and Karin Maier, Physica B **185**, 199 (1993).

Vita

2nd Lieutenant William A. Davis was born on 25 May 1971 in Latrobe, Pennsylvania. He graduated from Derry Area Senior High School in Derry, Pennsylvania in 1989 and attended Saint Vincent College in Latrobe, Pennsylvania graduating with a Bachelor of Science in Physics in May 1993. While attending Saint Vincent College, he was cross enrolled with AFROTC Detachment 730 at the University of Pittsburgh and Carnegie-Mellon University where he obtained a full three-year scholarship. He obtained a reserve commission in the USAF in May 1993. Shortly thereafter, he was assigned directly to the Air Force Institute of Technology School of Engineering to work on his Master of Science in Engineering Physics. His follow-on assignment from AFIT is to the Photonics Directorate at Rome Laboratory, Griffis AFB, NY.

Permanent Address: 919 Walnut Drive
Latrobe, PA 15650

REPORT DOCUMENTATION PAGE

Form Approved
OMB No. 0704-0188

1. AGENCY USE ONLY (Leave blank)	2. REPORT DATE	3. REPORT TYPE AND DATES COVERED
	December 94	Master's Thesis

4. TITLE AND SUBTITLE

Photoluminescence Spectroscopy of 4H- and 6H-SiC

5. FUNDING NUMBERS

6. AUTHOR(S)

2Lt. William A. Davis

7. PERFORMING ORGANIZATION NAME(S) AND ADDRESS(ES)

Air Force Institute of Technology
Department of Engineering Physics
Wright-Patterson AFB, OH 45433-6583

8. PERFORMING ORGANIZATION REPORT NUMBER

AFIT/GAP/ENP/94D-02

9. SPONSORING/MONITORING AGENCY NAME(S) AND ADDRESS(ES)

Dr. William Mitchel
Wright Laboratory, Materials Directorate
Wright-Patterson AFB, OH 45433-7707

10. SPONSORING/MONITORING AGENCY REPORT NUMBER

11. SUPPLEMENTARY NOTES

12a. DISTRIBUTION/AVAILABILITY STATEMENT

Approved for public release; distribution unlimited

12b. DISTRIBUTION CODE

13. ABSTRACT *(Maximum 200 words)*

Typical undoped bulk grown SiC shows n- or p-type conductivity due to residual impurities such as nitrogen, boron, or aluminum. In order to produce high resistivity material, vanadium can be used as a compensating dopant. Since vanadium is an amphoteric dopant in SiC, it produces either a donor state, $V_{Si}^{4+}(3d^1) \rightarrow V_{si}^{5+}(3d^0)$, or an acceptor state, $V_{Si}^{4+}(3d^1) \rightarrow V_{si}^{3+}(3d^2)$. Thus, vanadium doping can compensate both n- and p-type conductivity. In this work, vanadium doped and undoped 4H- and 6H-SiC grown by the sublimation method have been studied using low temperature photoluminescence (PL). It was found that the luminescence observed between 0.85 to 0.95 eV of the intra-3d-shell transition of $V_{si}^{4+}(3d^1)$ increased by an order of magnitude in samples intentionally doped with vanadium compared to samples unintentionally doped. In addition, the dominant visible-region luminescence was attributed to titanium which is an isoelectronic trap in SiC. The presence of a broad peak centered at ≈1.90 eV in some samples is believed to be attributed to donor-acceptor pair recombination between a Ti_{Si}-N_C complex donor and the boron defect complex acting as an acceptor. Finally, the Ti_{Si}-N_C complex donor location in the bandgap of 6H-SiC is estimated to be E_C-0.54 eV.

14. SUBJECT TERMS	15. NUMBER OF PAGES
Silicon Carbide, Wide-bandgap semiconductors, Photoluminescence	77
	16. PRICE CODE

17. SECURITY CLASSIFICATION OF REPORT	18. SECURITY CLASSIFICATION OF THIS PAGE	19. SECURITY CLASSIFICATION OF ABSTRACT	20. LIMITATION OF ABSTRACT
Unclassified	Unclassified	Unclassified	UL